Int. J. Cancer: **124,** 1429–1439 (2009)

Synergistic anti-tumor effect of paclitaxel with CRM197, an inhibitor of HB-EGF, in ovarian cancer

Hiroshi Yagi[1], Fusanori Yotsumoto[2], Kenzo Sonoda[1], Masahide Kuroki[4], Eisuke Mekada[3] and Shingo Miyamoto[4]*

[1]*Department of Obstetrics and Gynecology, Graduate School of Medical Sciences, Kyushu University, Fukuoka 812-8582, Japan*
[2]*Department of Obstetrics and Gynecology, School of Medicine, Fukuoka University, Fukuoka 814-0180, Japan*
[3]*Department of Cell Biology, Research Institute for Microbial Diseases, Osaka University, Osaka 565-0871, Japan*
[4]*Department of Biochemistry, Faculty of Medicine, Fukuoka University, Fukuoka 814-0180, Japan*

Heparin-binding EGF-like growth factor (HB-EGF) plays a pivotal role in tumor growth and clinical outcomes in patients with ovarian cancer, leading to the validation of HB-EGF as a target for ovarian cancer therapy. In this study, we investigated the anti-tumor effects of paclitaxel, as an anti-cancer agent, and CRM197, as a specific inhibitor off HB-EGF, in ovarian cancer. Paclitaxel induced transient ERK activation and sustained activation of JNK and p38 MAPK through the ectodomain shedding of HB-EGF in SKOV3 cells. In addition, the overexpression of HB-EGF in paclitaxel-treated SKOV3 cells resulted in modulation of paclitaxel-evoked MAPK signaling, including marked activation of ERK and Akt, and minimized activation of JNK and p38 MAPK, indicating that HB-EGF is involved in drug sensitivity through the balance of anti-apoptotic and pro-apoptotic signals induced by paclitaxel. The combination of paclitaxel with CRM197 had an inhibitory effect on cell proliferation and enhanced apoptosis *via* the inhibition of ERK and Akt activation and the stimulation of p38 and JNK activation. More prominently, the administration of paclitaxel with CRM197 resulted in synergistic anti-tumor effects in SKOV3 cells and in SKOV3 cells overexpressing HB-EGF in xenografted mice. Accordingly, inhibitory agents against HB-EGF, such as CRM197, represent possible chemotherapeutic and chemosensitizing agents for ovarian cancer.

Key words: CRM197; HB-EGF; paclitaxel; EGFR; ovarian cancer

Paclitaxel was originally isolated from the bark of *Taxus brevifolia*,[1] and has been widely used as a therapeutic agent for various cancers including ovarian, breast and lung cancers[2,3] Although this agent has been known to promote the assembly of microtubules from tubulin and inhibits their depolymerization both *in vitro* and *in vivo*, it is unknown how paclitaxel causes its anti-tumor effects in human cancers. Since paclitaxel induces apoptosis in a variety of cancer cells through the activation or suppression of MAPK (mitogen-activating protein kinase) family molecules, including extracellular signal-regulated kinases (ERK1/2), p38 MAPK and Jun-terminal kinases (JNK)[4,5] it is plausible that the MAPK signaling pathways are involved in the cellular responses to paclitaxel during cancer therapy.

Heparin-binding EGF (epidermal growth factor)-like growth factor (HB-EGF) is an EGFR (epidermal growth factor receptor) ligand.[6] HB-EGF is initially synthesized as a transmembrane protein, similar to other members of the EGF family of growth factors.[7] The membrane-anchored form of HB-EGF (proHB-EGF) is cleaved at the cell surface by a protease to yield the soluble form of HB-EGF (sHB-EGF) *via* a mechanism known as ectodomain shedding.[8] Members of the ADAM (a disintegrin and metalloprotease) family, such as ADAM9, ADAM10, ADAM12 and ADAM17, or other metalloproteases, are involved in this process.[9] A variety of signaling pathways are thought to be activated following the ectodomain shedding of HB-EGF.[10,11] Ectodomain shedding of proHB-EGF, itself, is induced by various stimuli including phorbol ester TPA, calcium ionophre and various growth factors and cytokines.[12–14] Ras-Raf-MEK (MAPK kinase) and Protein kinase C (PKC) are involved in the intracellular signaling pathway for proHB-EGF processing.[8,15] sHB-EGF is a potent mitogen and chemoattractant for a number of different cell types; thus, ectodomain shedding is critical for HB-EGF growth factor activity.[16–19]

Increasing evidence suggests a critical role for HB-EGF in ovarian cancer cell growth and tumor progression: Among members of the EGFR family of growth factors, HB-EGF gene expression in cancerous tissues and HB-EGF protein levels were shown to be significantly elevated in patients' ascites.[20,21] In addition, tumor formation by human ovarian cancer cell lines was enhanced by exogenous expression of proHB-EGF, and completely blocked by proHB-EGF gene RNA interference or by CRM197, a specific HB-EGF inhibitor.[20] CRM197 is a nontoxic mutant of diphtheria toxin shares immunological properties with the native molecule. CRM197 binds to human HB-EGF and blocks its mitogenic activity, due to prohibition of EGFR binding.[22] In patients with ovarian cancer, high expression of HB-EGF is significantly associated with poor clinical outcome.[23] Cancer cells with elevated expression of HB-EGF are also resistant to paclitaxel.[20] According to these studies, HB-EGF is a promising target for ovarian cancer therapy and the expression of HB-EGF is of relevance to drug-sensitivity in patients with ovarian cancer.

In this study, we showed that the anti-tumor effect of paclitaxel was abrogated by enhanced expression of HB-EGF using the ovarian cancer cell line SKOV3. Paclitaxel induced the ectodomain shedding of HB-EGF, resulting in the activation of anti-apoptotic signals, including ERK and Akt, and the attenuation of pro-apoptotic signals, including JNK and p38 MAPK. Therefore, cancer cells with elevated expression of HB-EGF have properties involved in resistance to paclitaxel. The suppression of HB-EGF function in cancer cells promoted the anti-tumor effect of paclitaxel in ovarian cancer.

Material and methods

Reagents and antibodies

Diphtheria toxin (DT) and CRM197 were prepared as described previously.[24] Paclitaxel was partly obtained from Calbiochem (San Diego, CA) and kindly provided by Bristol Pharmaceuticals K. K. (Tokyo, Japan). GM6001 (an inhibitor for metalloprotease), U0126 (an inhibitor for MEK), SP600125 (an inhibitor for JNK) and SB203580 (an inhibitor for p38 MAPK) were purchased from Calbiochem (San Diego, CA). siRNAs for ADAM9, ADAM10, ADAM12 and ADAM19 were purchased from TaKaRa Bio

---

The first two authors contributed equally to this work.

Additional Supporting Information may be found in the online version of this article.

Grant sponsor: Scientific Research on Priority Areas; Grant number: 19591947; Grant sponsors: Fukuoka University Research Foundation, Ministry of Education, Culture, Sports, Science and Technology.

***Correspondence to:** Department of Biochemistry, Faculty of Medicine, Fukuoka University, 7-45-1, Nanakuma, Jonan-ku, Fukuoka 814-0180, Japan. Fax: 81-92-801-3600.
E-mail: smiya@cis.fukuoka-u.ac.jp

Received 30 April 2008; Accepted after revision 11 September 2008
DOI 10.1002/ijc.24031
Published online 30 September 2008 in Wiley InterScience (www.interscience.wiley.com).

(Shiga, Japan). TransIT-TKO transfection reagent was purchased from Mirus (Madison, EI). Recombinant human HB-EGF and polyclonal antibody against HB-EGF were purchased from R&D Systems (Minneapolis, MN). Polyclonal antibodies against EGFR, ERK and ADAM17, and monoclonal antibodies against p38 MAPK and JNK were purchased from Santa Cruz Biotechnology (Santa Cruz, CA). Polyclonal anti-phospho-p38 MAPK was obtained from GT (Minneapolis, MN). Polyclonal anti-phospho-JNK, monoclonal anti-phospho-ERK and anti-phosphotyrosine antibodies were purchased from Upstate Biotechnology (Lake Placid, NY). Polyclonal anti-Akt and monoclonal anti-phospho-Akt (Ser473) antibodies were obtained from Cell Signaling Technology (Beverly, MA). Monoclonal anti-β-actin antibody was purchased from Sigma (St Louis, MO). FITC-conjugated anti-goat IgG and peroxidase-conjugated anti-mouse IgG antibodies were obtained from Amersham Corp. (Arlington Heights, IL). Peroxidase-conjugated anti-rabbit IgG antibody was obtained from Zymed (San Francisco, CA), respectively.

Plasmid construction and transfection

The construction of plasmids encoding a human pro-HB-EGF cDNA and an uncleavable mutant inserted into the eukaryotic expression vector pRc/CMV (Invitrogen, Carlsbad, CA) has been described previously.[25] Plasmids expressing HB-EGF short interfering RNA (siRNA) (pH1-PUR/siRNA HB-EGF) were prepared as described previously.[20,26] Transfection of all constructs into SKOV3 cells was performed using LipofectAMINE 2000 reagent (Invitrogen, Carlsbad, CA), according to the manufacturer's instructions. Transfected cells were selected with 400 μg/ml of G418 or 5 μg/ml of puromycin and had already been established previously.[20] SK-HB-1 cells, which were obtained by transfecting SKOV3 cells with proHB-EGF, overexpressed proHB-EGF on the cell surface. SK181-1 cells were proHB-EGF knock-down cells derived from SKOV3 cells, and SK-MHB-1 cells were SKOV3 cells transfected with an uncleavable proHB-EGF mutant.

siRNA transfection

Cells (5×10^5) were seeded on poly-lysine-coated 10-cm dishes (50–60% confluence). The siRNAs were individually transfected into cells using TransIT-TKO according to the manufacturer's instructions. The final concentration of each siRNA for transfection was 25 nM. After incubation for 48 hr, the cells were subjected to apoptosis assays.

RNA extraction, cDNA synthesis and polymerase chain reaction

RNA was extracted using TRIzol (Invitrogen, Carlsbad, CA), according to the manufacturer's protocol. First-strand cDNA synthesis was performed with 1 μg of total RNA using Superscript™ II reverse transcriptase (Invitrogen), following the manufacturer's protocol. The TaqMan quantitative polymerase chain reaction (PCR) reaction was carried out using the sequences of the oligonucleotide primer pairs and TaqMan probes for each ADAM family and glyceraldehyde-3-phosphate dehydrogenase (GAPDH) as previously described.[23] Experiments were carried out independently 3 times. To examine the expression of ADAM9, ADAM10, ADAM12 or GAPDH in ovarian cancer, reverse transcriptase PCR (RT-PCR) analysis was performed using primers specific ADAM9 (94°C for 15 sec, 45°C for 30 sec, 68°C for 60 sec, 30 cycles: sense 5′-GGA GCA TCG GGT TCC A-3′, antisense 5′-GCT TTC CAC ACA AAG CA-3′), ADAM10 (94°for 15 sec, 45°C for 30 sec, 68°C for 60 sec, 30 cycles: sense 5′-CTG TTA ACC CGT GAG GA-3′, antisense 5′-ACA CCA GTC ATC TGG TA-3′), ADAM12 (94°C for 15 sec, 47°C for 30 sec, 68°C for 60 sec, 30 cycles: sense 5′-ACA CAC ACG GGG GGA A-3′, antisense 5′-TCA GTA CCG TCT TGC AGA-3′), ADAM17 (94°C for 15 sec, 47°C for 30 sec, 68°for 60 sec, 30 cycles: sense 5′-CCC CGA ATG AGG ACC A-3′, antisense 5′-AGG GCT TTC CTT TCC TCA -3′ or GAPDH (94°for 15 sec, 48°C for 30 sec, 68°C for 60 sec, 30 cycles: sense 5′-ACCCAGAAGACTGTG-GATGG-3′, antisense 5′-TGCTGTAGCCAAATTCGTTG-3′). Experiments were independently carried out 3 times.

Cell culture

SKOV3 cells and transfected cells including SK-HB-1, SK-181-1 and SK-MHB-1 cells were maintained in RPMI 1640 supplemented with 100 units /ml penicillin G, 100 μg/ml streptomycin and 10% fetal bovine serum (ICN Biomedical, Irvine, CA). Another human ovarian cancer cell line, OVMG1, which was established in our department from a surgical specimen of serous adenocarcinoma of the ovary, was also maintained in RPMI1640 suppelmented with 100 untis/ml penicillin G, 100 mg/ml streptomycin and 10% fetal bovine serum (ICN Biomedical, Irvine, CA).[27]

Flow cytometry, diphtheria toxin binding assay and protein tyrosine phosphorylation

Cells were detached with trypsin-EDTA, and then allowed to recover for 30 min in RPMI 1640 containing 10% fetal bovine serum. Cells were incubated with polyclonal anti-HB-EGF antibody for 30 min at 4°C and then with FITC-conjugated anti-goat IgG antibody for 30 min at 4°C. The positive cells were quantified by flow cytometric analysis (Becton Dickinson, FACSculibar, Franklin Lakes, NJ). To assess the effect of each pharmacologic agent on DT binding, after rinsing with serum-free medium, cells (1×10^6) were seeded on poly-lysine-coated 6-cm dishes to prohibit interactions mediated by adhesion molecules, such as integrins and cadherins. Cells were incubated with RPMI 1640 plus 10% fetal bovine serum in the presence of various concentrations of paclitaxel and/or other pharmacological agents at 37°C, after assuring complete adherence of the cells to the poly-lysine-coated dishes. Binding of ^{125}I-labeled DT to cells was measured as described previously, and values of specific binding were determined.[28] To examine the expression of ERK and other signaling molecules, cells were rinsed in phosphate-buffered saline containing 1 mM sodium orthovanadate and then lysed in immunoprecipitation assay buffer (1% Triton X-100, 1% sodium deoxycholate, 0.1% SDS, 150 mM NaCl, 50 mM Tris (pH 8.0), 0.2 unit/ml aprotinin, 2 μg/ml leupeptin, 1 μg/ml pepstatin A, 2 mM phenylmethylsulfonyl fluoride and 1 mM sodium orthovanadate). Extracts and immunoprecipitants were then subjected to SDS-PAGE and immunoblotting analysis. The expression of phosphorylated proteins by immunoblotting was quantified by densitometric analysis, using a Fuji image analyzer LAS mini-3000 and Multi-Gauge software. The expression ratio of relative band intensity for the phosphorylated protein was calculated from densitometric analysis. The strongest band among the phosphorylated proteins in each experiment was defined as 100 % of band intensity. When no definite signal of band was detected by densitometry, the expression ratio was determined as 0 % of band intensity. The mean value is shown as a representative value for the expression ratios of band intensity in 3 experiments and the mean value of strongest band in the experiment results in 100% of band intensity.

The amount of soluble HB-EGF in culture medium

Cells were seeded on 6-cm dishes (50–60% confluence) and incubated in media containing serum with 10 μM of paclitaxel for 0, 1, 3 or 6 hr. Transfected cells with siRNA for ADAMs were also seeded on 6-cm dishes (50–60% confluence) and incubated in media containing serum with 100 nM of paclitaxel for 48 hr. After that, each culture medium (CM) and the soluble forms of HB-EGF bound to extracellular matrices on the cell surface supernatant (CSS) were completely collected according to the following procedures.[29] First, CM was collected. After that, cells were gently agitated with 2 ml of 2M NaCl, and then the supernatant was collected. After the cells were washed at 3 times with 2 ml of Washing Buffer (1 mg/ml bovine serum albumin in PBS), the total 6 ml of washing buffer were collected and mixed with 2 ml supernatant

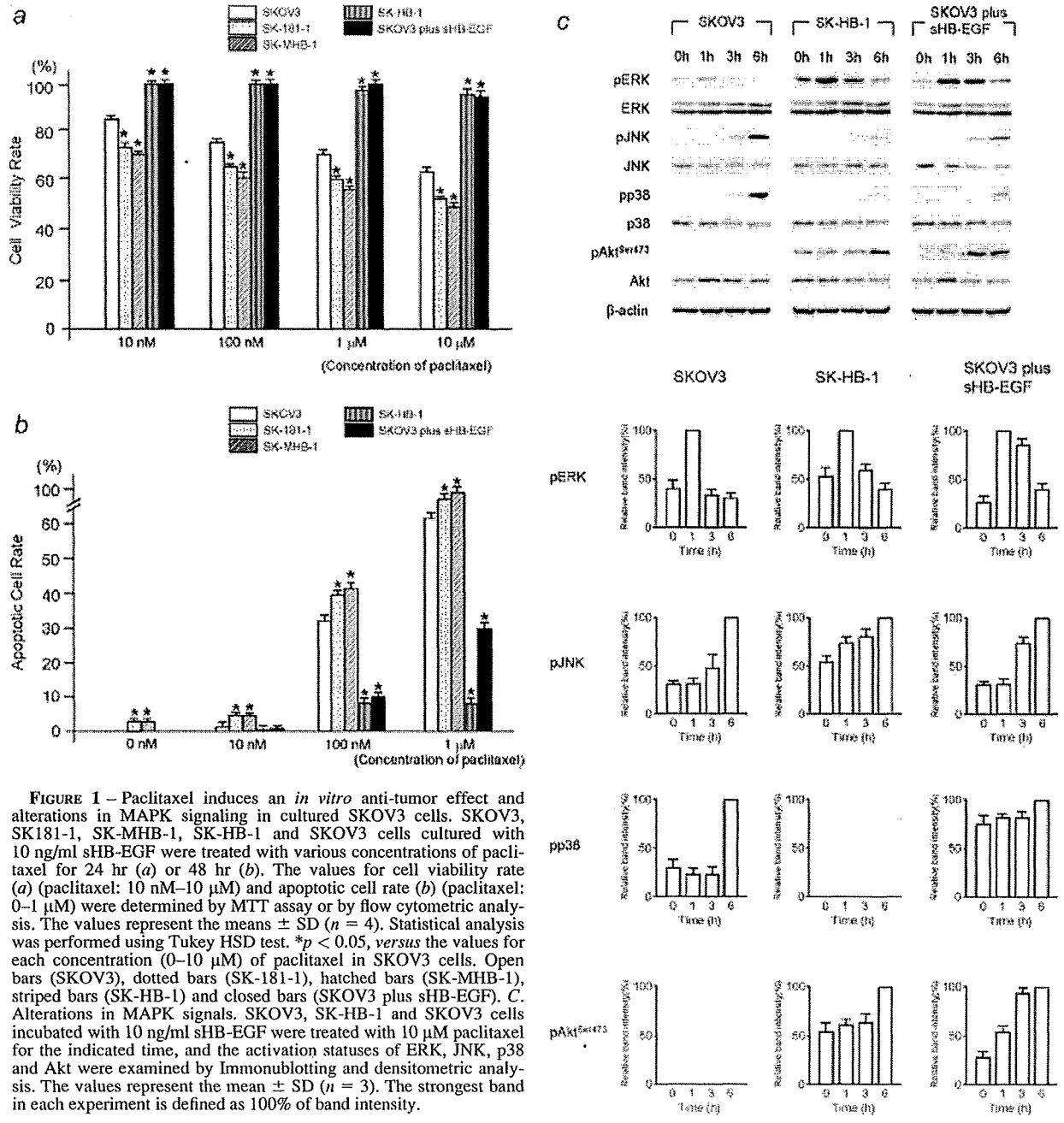

FIGURE 1 – Paclitaxel induces an *in vitro* anti-tumor effect and alterations in MAPK signaling in cultured SKOV3 cells. SKOV3, SK181-1, SK-MHB-1, SK-HB-1 and SKOV3 cells cultured with 10 ng/ml sHB-EGF were treated with various concentrations of paclitaxel for 24 hr (*a*) or 48 hr (*b*). The values for cell viability rate (*a*) (paclitaxel: 10 nM–10 μM) and apoptotic cell rate (*b*) (paclitaxel: 0–1 μM) were determined by MTT assay or by flow cytometric analysis. The values represent the means ± SD ($n = 4$). Statistical analysis was performed using Tukey HSD test. $*p < 0.05$, *versus* the values for each concentration (0–10 μM) of paclitaxel in SKOV3 cells. Open bars (SKOV3), dotted bars (SK-181-1), hatched bars (SK-MHB-1), striped bars (SK-HB-1) and closed bars (SKOV3 plus sHB-EGF). *C*. Alterations in MAPK signals. SKOV3, SK-HB-1 and SKOV3 cells incubated with 10 ng/ml sHB-EGF were treated with 10 μM paclitaxel for the indicated time, and the activation statuses of ERK, JNK, p38 and Akt were examined by Immonublotting and densitometric analysis. The values represent the mean ± SD ($n = 3$). The strongest band in each experiment is defined as 100% of band intensity.

FIGURE 1 – CONTINUED.

as CSS. The level of HB-EGF in CM or CSS was examined using ELISA. The amount of soluble HB-EGF in culture medium was calculated as the sum of 2 values of CM and CSS. The levels of HB-EGF were determined using a commercially available sandwich ELISA kit (DuoSet Kit; R&D System, Minneapolis, MN) in accordance with the manufacturer's instructions. All experiments were conducted in triplicate and the mean HB-EGF value was regarded as the representative value of HB-EGF in each case.

Cell viability and cell apoptosis assays

Cells (2×10^4) were treated as in the DT-binding assay and then seeded on polylysine-coated 96-well dishes. To assess the cell viability, cells were incubated with 200 μl of RPMI 1640 plus 10% fetal bovine serum at 37°C for 24 h in the presence of taxol (10 nM–10 μM) and/or 1 μg/ml CRM197. The MTT assay is a colorimetric assay that relies on the ability of viable cell to convert a soluble tetrazolium salt, 3-(4,5-dimethyl-2-tetrazolyl)-2,5-diphenyl-2H tetrazolium bromide (MTT), into a formazan precipitate, causing a yellow-to purple color change. The MTT assay was then performed according to the manufacturer's instructions (Roche Diagnostics GmbH, Mannheim, Germany). Each experi-

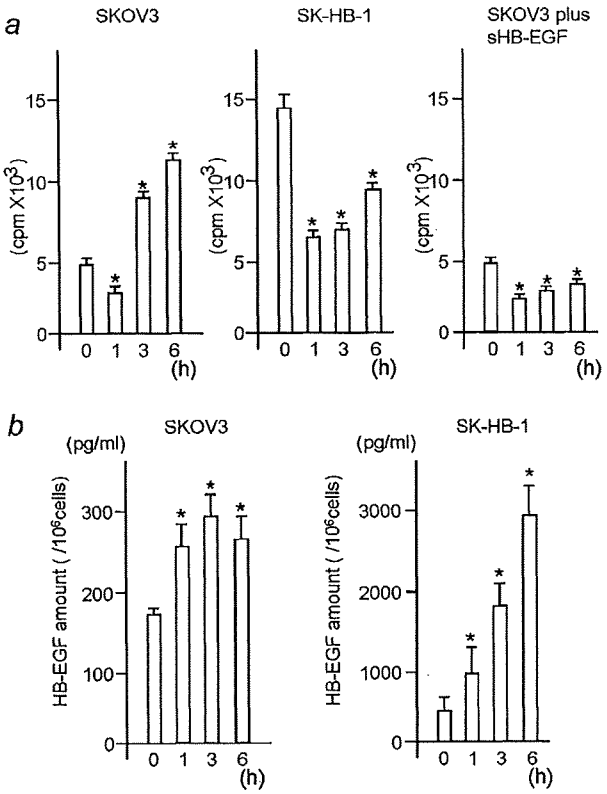

FIGURE 2 – Effect of paclitaxel and various pharmacological inhibitors on the ectodomain shedding of HB-EGF, tyrosine phosphorylation of EGFR and phosphorylation of ERK. (*a*) Alteration in ectodomain shedding of HB-EGF mediated by paclitaxel. SKOV3, SK-HB-1 and SKOV3 cells incubated with 10 ng/ml of sHB-EGF were incubated with paclitaxel (10 μM) for the indicated time, and the amount of proHB-EGF on the cell surface was determined by a diphtheria toxin-binding assay. The values represent the means ± SD ($n = 4$). Statistical analysis was performed using Tukey HSD test. *$p < 0.05$, *versus* the values at 0 hr in each of the cell types. (*b*) Alteration in the amount of soluble form of HB-EGF in culture medium. SKOV3 and SK-HB-1 cells were incubated with paclitaxel (10 μM) for the indicated time, and the amount of soluble form of HB-EGF in culture medium was determined using ELISA. The values represent the means ± SD ($n = 4$). Statistical analysis was performed using Tukey HSD test. *$p < 0.05$, *versus* the values at 0 hr in each of the cell types. (*c*), (*d*), (*e*) and (*f*) (upper panel). Effect of various pharmacological inhibitors on the ectodomain shedding of HB-EGF induced by paclitaxel. SKOV3 (*c*), SK-HB-1 (*d*), SK181-1 (*e*) and SK-MHB-1 (*f*) cells were incubated with paclitaxel (10 μM) in the presence or absence of GM6001 (5 μM) or U0126 (10 μM) for 1 hr, and the amount of proHB-EGF on the cell surface was determined. The values represent the mean ± SD ($n = 4$). Statistical analysis was performed using Tukey HSD test. *$p < 0.05$, *versus* values in the absence of paclitaxel and any pharmacological agents in each of the cell types. The phosphorylation statuses of EGFR and ERK (lower panel) were examined by immunoblotting and densitometric analysis. The values represent the mean ± SD ($n = 3$). The strongest band in each experiment is defined as 100% of band intensity.

ment was conduced in triplicate. The mean value is shown as the representative value for each experiment. The cell viability rate was calculated as each mean value divided by the mean value in the MTT assay in the absence of taxol and CRM197. In the cell apoptotic assay, cells (1×10^5) were treated as aforementioned and seeded on poly-lysine-coated 6-cm dishes. Thereafter, the medium was replaced with RPMI 1640 containing 10% fetal bovine serum at 37°C for 48 hr in the presence of taxol (10 nM–1 μM) and/or 1 μg/ml CRM197, with or without each pharmacological agent, after assuring the complete adherence of the cells to the poly-lysine-coated 6-cm dishes. Cells were incubated with TdT reaction reagent for 1 hr at 37°C, according to the manufacturer's recommended protocol (MEBSTAIN Apoptosis Kit Direct, MBL, Japan). TUNEL-positive cells were quantified as apoptotic cells by flow cytometric analysis (Becton Dickinson, FACScalibur, Franklin Lakes, NJ).[21] The proportion of TUNEL-positive cells was calculated as the apoptotic cell rate, and the mean value is shown as a representative value for each experiment. Each experiment was conducted in triplicate.

Tumor growth in nude mice

Subconfluent cell cultures were detached from plates with trypsin-EDTA. A total volume of 250 μl containing 5×10^6 cells suspended in serum-free RPMI 1640 was injected subcutaneously into female BALB/c nu/nu mice at 5 weeks of age (Charles River Laboratories, Japan). Injected mice were examined every week for tumor apparition. Tumor volume was calculated as described previously.[20] To assess the anti-tumor effects of paclitaxel and/or CRM197, CRM197 or paclitaxel was dissolved in 20 mM HEPES and 150 mM NaCl (pH 7.2), or in equal volumes of absolute ethanol and Cremophor EL. The indicated amount of CRM197 and/or paclitaxel was injected intraperitoneally into tumor-bearing mice each week. All experimental use of animals complied with the guidelines of Animal Care of Kyushu University and Fukuoka University.

Statistical analysis

Data for the two experiments were analyzed using the Mann-Whitney *U* test. $p < 0.05$ was considered statistically significant. Data for many of the experiments were analyzed using Tukey HSD test. Statistical significance was also set at $p < 0.05$.

Results

The relationship between the in vitro *anti-tumor effects of paclitaxel or paclitaxel-induced MAPK signaling and HB-EGF expression*

To evaluate the *in vitro* anti-tumor effect of paclitaxel involved in HB-EGF expression, the cell viability rate or apoptotic cell rate in the presence of paclitaxel (0–10 μM) was examined in SKOV3, SK-181, SK-MHB-1 and SK-HB-1 cells. Compared to the expression of SKOV3 cells as the parental cells, SK-HB-1 cells or SK-181-1 cells are regarded as the cells harboring high or low expression of HB-EGF, respectively (Supp. Info. Fig. 1). SK-MHB-1 cells have overexpression of uncleaved proHB-EGF. In SK-MHB-1 cells, the soluble form of HB-EGF is little secreted in culture medium, due to blockage of ectodmain shedding of pro-HB-EGF (Supp. Info. Fig. 1). Therefore, SK-MHB-1 cells are considered as another type of cells harboring low expression of HB-EGF. In SKOV3, SK-181-1 and SK-MHB-1 cells, paclitaxel suppressed cell viability and augmented the number of apoptotic cells in dose-dependent manners, while no significant *in vitro* anti-tumor effects on cell viability or apoptosis were found in SK-HB-1 cells or SKOV3 cells cultured with a soluble form of HB-EGF (sHB-EGF), even at the highest concentration of paclitaxel (Figs. 1*a* and 1*b*). In SK-181-1 and SK-MHB-1 cells, the rate of cell viability was suppressed and the number of apoptotic cells was augmented, compared with those in SKOV3 cells. The exact numbers of apoptotic SKOV3, SK-181-1 and SK-MHB-1 cells treated with 10 μM of paclitaxel for 48 hr could not be examined, because many of these cells were detached from the dishes. There was a significant difference between SK-HB-1 and SKOV3 plus sHB-EGF with respect to apoptotic rate in response to 1 μM paclitaxel (8 *vs.* 29%). The cell viability rate or cell apoptotic rate was examined for 24 or 48 hr. The extension of incubation time might result in the degradation of sHB-EGF, leading to its loss-of-function. These results indicate that the *in vitro* anti-tumor effects mediated by paclitaxel are modulated by HB-EGF expression.

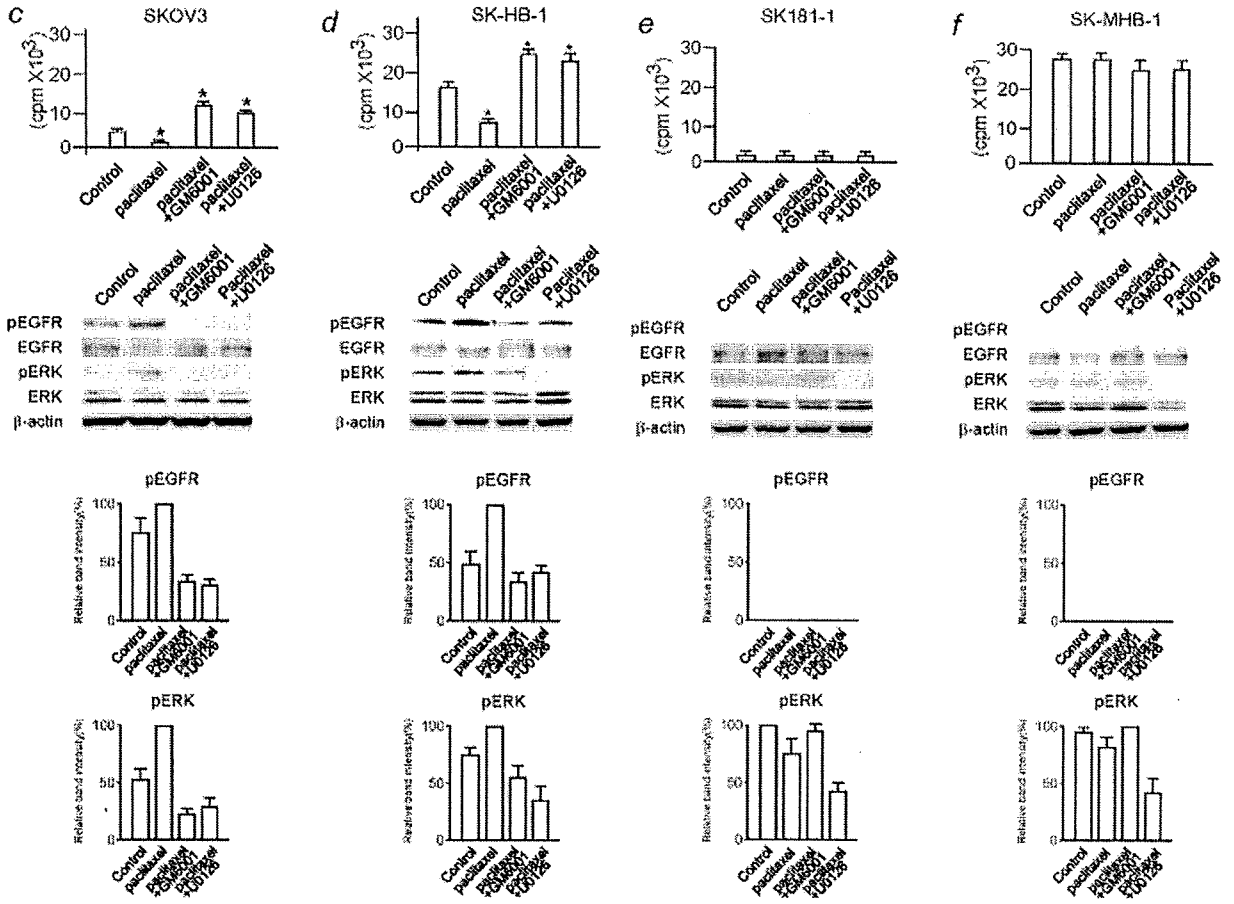

FIGURE 2 – CONTINUED.

To investigate the time course of the alterations in MAPK activity induced by paclitaxel, the activities of ERK, p38 MAPK, JNK and Akt in the presence of 10 μM of paclitaxel were examined in SKOV3, SK-HB-1 and SKOV3 cells cultured with sHB-EGF. In SKOV3 cells, ERK was transiently activated at 1 hr after paclitaxel added, but this activated state was not observed at 3 and 6 hr (Fig. 1*c*). In SK-HB-1 cells and SKOV3 cells cultured with sHB-EGF, the addition of paclitaxel markedly activated ERK, and the activation of ERK was sustained until 6 hr after the addition of paclitaxel (Fig. 1*b*). In contrast to the marked activation of JNK and p38 MAPK at 6 hr after the addition of paclitaxel in SKOV3 cells, the activation of JNK and p38 MAPK was minimized in SK-HB-1 cells and SKOV3 cells cultured with sHB-EGF (Fig. 1*c*). An increased activation of Akt over time was seen in SK-HB-1 cells and SKOV3 cells cultured with sHB-EGF, but no significant activation of Akt was detected in SKOV3 cells following the addition of paclitaxel (Fig. 1*c*). In SKOV3 cells, the activation of JNK at 6 hr after the addition of pacitaxel was blocked by the presence of JNK inhibitor (SP600125), but not p38 MAPK inhibitor (SB203580) or MEK inhibitor (U0126) (Supp. Info. Fig. 2). In SKOV3 cells, the phosphorylation of p38 MAPK at 6 hr after the addition of paclitaxel was also suppressed by the presence of p38 MAPK inhibitor, but not JNK inhibitor or MEK inhibitor. In SK-HB-1 cells, the activation of Akt at 6 hr after the addition of paclitaxel was little inhibited by the presence of JNK inhibitor or p38 MAPK inhibitor (Supp. Info. Fig. 2). These results indicate that the enhanced expression of HB-EGF modulates paclitaxel-induced MAPK signaling.

Paclitaxel induces the ectodomain shedding of HB-EGF

To confirm the ectodomain shedding of proHB-EGF mediated by paclitaxel, the expression of proHB-EGF was measured using a DT binding assay. In SKOV3 cells, the amount of proHB-EGF on the cell surface transiently decreased and then increased over time following treatment with 10 μM paclitaxel. In SK-HB-1 cells and SKOV3 cells incubated with sHB-EGF, paclitaxel treatment resulted in a prolonged decrease in the amount of proHB-EGF at the cell surface (Fig. 2*a*). In SKOV3 cells, the amount of sHB-EGF in culture medium significantly increased at 1 hr, compared to that at 0 hr (Fig. 2*b*). No significant increase was found after 1 hr. On the other hand, In SK-HB-1 cells, the amount of sHB-EGF in culture medium continued to increase for 6 hr (Fig. 2*b*). These results indicated that the cleavage of proHB-EGF in the presence of paclitaxel is sustained by the enhanced expression of HB-EGF.

To assess the association between the alterations in signaling and ectodomain shedding of proHB-EGF in the presence of paclitaxel, the activation of EGFR as well as ERK and expression of proHB-EGF on cell surface were examined in SKOV3, SK-HB-1, SK-181-1 and SK-MHB-1 cells. Paclitaxel induced the tyrosine phosphorylation of EGFR as well as the activation of ERK in SKOV3 and SK-HB-1 cells (Figs. 2*c* and 2*d*). A metalloprotease inhibitor, GM6001, which inhibits the ectodomain shedding of proHB-EGF, and a MEK inhibitor, U0126, abrogated the paclitaxel-induced cleavage of proHB-EGF as well as the activation of EGFR and ERK in SKOV3 and SK-HB-1 cells, whereas ectodo-

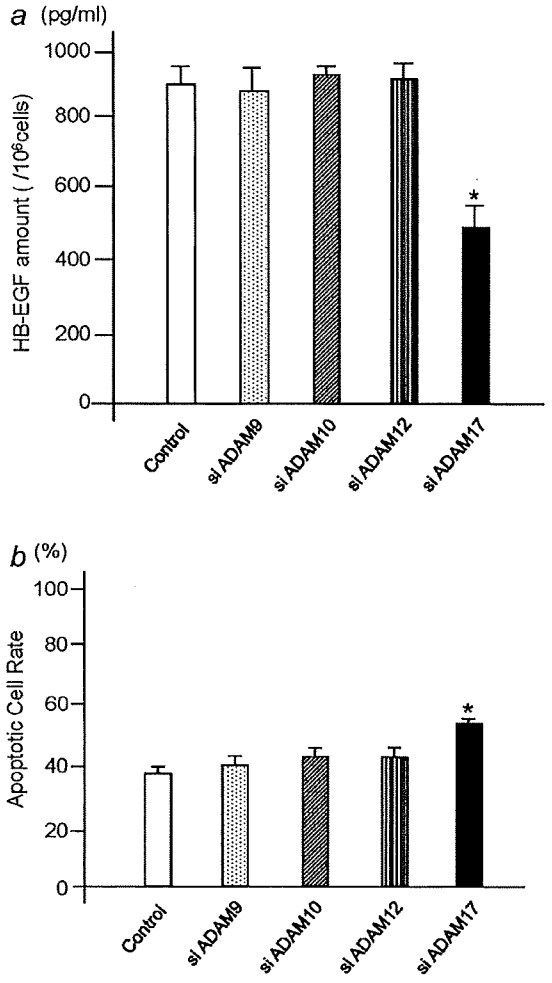

FIGURE 3 – Involvement of ADAM17 in ectodomain shedding mediated by paclitaxel. Untransfected SKOV3 cells or SKOV3 cells transfected with siRNAs against ADAM9, ADAM10, ADAM12 or ADAM17 were incubated in culture medium containing serum with paclitaxel (100 nM) for 48 hr. The amounts of secreted HB-EGF (*a*) and the values for apoptotic cell rate (*b*) were determined by ELISA or by flow cytometric analysis. The values represent the means ± SD ($n = 4$). Statistical analysis was performed using Tukey HSD test. $^*p < 0.05$, *versus* the values of untransfected SKOV3 cells as a control. Open bars (untransfected), dotted bars (siADAM9), hatched bars (siADAM10), striped bars (siADAM12), and closed bars (siADAM17).

main shedding of proHB-EGF or activation of EGFR and ERK was little found in SK181-1 and SK-MHB-1 cells (Figs. 2*c*–2*f*). The addition of JNK inhibitor SP600125 or the p38 MAKP inhibitor SB203580 did not prohibit the cleavage of proHB-EGF in SKOV3 cells or SK-HB-1 cells (Supp. Info. Fig. 3). These results indicate that the paclitaxel-induced activation of ERK and EGFR, but not the activation of JNK or p38 MAPK, requires the ectodomain shedding of proHB-EGF.

Blockade of ectodamin shedding of HB-EGF affects paclitaxel-induced apoptosis

To gain insight into the relationship between the cleavage of pro-HB-EGF and the apoptosis induced by paclitaxel, the amount of HB-EGF secreted into the medium and the numbers of apoptotic cells were examined in cultures of untransfected SKOV3 cells and SKOV3 cells transfected with siRNAs against ADAM9, ADAM10, ADAM12 or ADAM17. ADAM17 was abundantly expressed n SKOV3, SK-HB-1, SK-181-1 and SK-MHB-1 cells, compared to the expression of other ADAMs (Supp. Info. Fig. 4A). The transfection of siRNA for each ADAM significantly suppressed the expression of ADAM (Supp. Info. Fig. 4). The amount of sHB-EGF was decreased only in the medium of ADAM17 knock-down cells compared with SKOV3 cells (Fig. 3*a*). Suppression of ADAM17 augmented the number of apoptotic cells, whereas no significant apoptosis was observed in untransfected SKOV3 cells or SKOV3 cells transfected with siRNAs against ADAM9, ADAM10 or ADAM12 (Fig. 3*b*).

CRM197 acts in collaboration with paclitaxel in causing anti-tumor effects

To further address the anti-tumor effects of paclitaxel and CRM197, cell viability rate, cell apoptosis and alterations in MAPK signaling were examined in SKOV3 cells and SK-HB-1 cells. The cell viability rate of SKOV3 cells in the presence of both paclitaxel and CRM197 was strongly inhibited, compared with that only in the presence of paclitaxel (Fig. 4*a*). In SK-HB-1 cells, cell viability was barely inhibited with paclitaxel alone, but it was inhibited in the presence of both paclitaxel and CRM197, as seen in SKOV3 cells. In SKOV3 and SK-HB-1 cells, significant apoptosis was seen in cells treated with a combination of paclitaxel and CRM197, compared with cells treated with paclitaxel only (Fig. 4*b*).The exact number of apoptotic SKOV3 cells treated with 10 μM of paclitaxel for 48 hr could not be examined, because many of the SKOV3 cells were detached from the dishes. In the presence of CRM197, the activation of EGFR and ERK was completely blocked after 1 and 6 hr of paclitaxel treatment in SKOV3 and SK-HB-1 cells (Fig. 4*c*). Conversely, p38 MAPK and JNK in SKOV3 and SK-HB-1 cells were significantly activated at 6 hr in the presence of paclitaxel and CRM197, compared with those in the presence of paclitaxel alone (Fig. 4*c*). In addition, the combination of paclitaxel and CRM197 more significantly suppressed the activation of Akt than paclitaxel alone in SK-HB-1 cells (Fig. 4*c*). The numbers of apoptotic SKOV3 and SK-HB1 cells in the presence of paclitaxel plus SP600125 or SB203580 were significantly lower than those in the presence of paclitaxel alone, indicating that the activation of JNK or p38 MAPK is implicated in apoptosis induced by paclitaxel (Fig. 4*d*). In addition, the blockade of ERK signaling by U0126 resulted in an increase in paclitaxel-induced apoptosis (Fig. 4*d*). These results suggested that CRM197 suppressed the anti-apoptotic signals mediated by ERK and Akt and enhanced the pro-apoptotic signals JNK and p38 MAPK.

Paclitaxel and CRM197 synergistically inhibit tumor formation in vivo

To elucidate the *in vivo* anti-tumor effects of paclitaxel and CRM197, alone or in combination, tumor formation in xenografted mice was continuously measured after inoculation with SKOV3 and SK-HB-1 cells. When CRM197 was administered alone, tumor growth in mice was suppressed in a dose-dependent manner in both cell lines; it was partially suppressed by 5 mg/kg CRM197 and completely suppressed by 50 mg/kg CRM197 (Figs. 5*a* and 5*b*). Administration of paclitaxel (20 mg/kg) suppressed tumor formation by SKOV3 cells, whereas the tumor growth by SK-HB-1 cells was not inhibited (Figs. 5*c* and 5*d*), indicating that HB-EGF is of relevance to the resistance to paclitaxel. No inhibition of tumor formation in SKOV3 cells or SK-HB-1 cells was found when mice were treated with paclitaxel (10 mg/kg) alone (Figs. 5*c* and 5*d*). However, co-administration of 10 mg/kg paclitaxel and 5 mg/kg CRM197 completely blocked tumor formation by both SKOV3 cells and SK-HB-1 cells (Figs. 5*e* and 5*f*). In OVMG1 cells, tumor formation was also completely blocked by co-administration of 10 mg/kg paclitaxel and 5 mg/kg CRM197 (Fig. 5*g*).

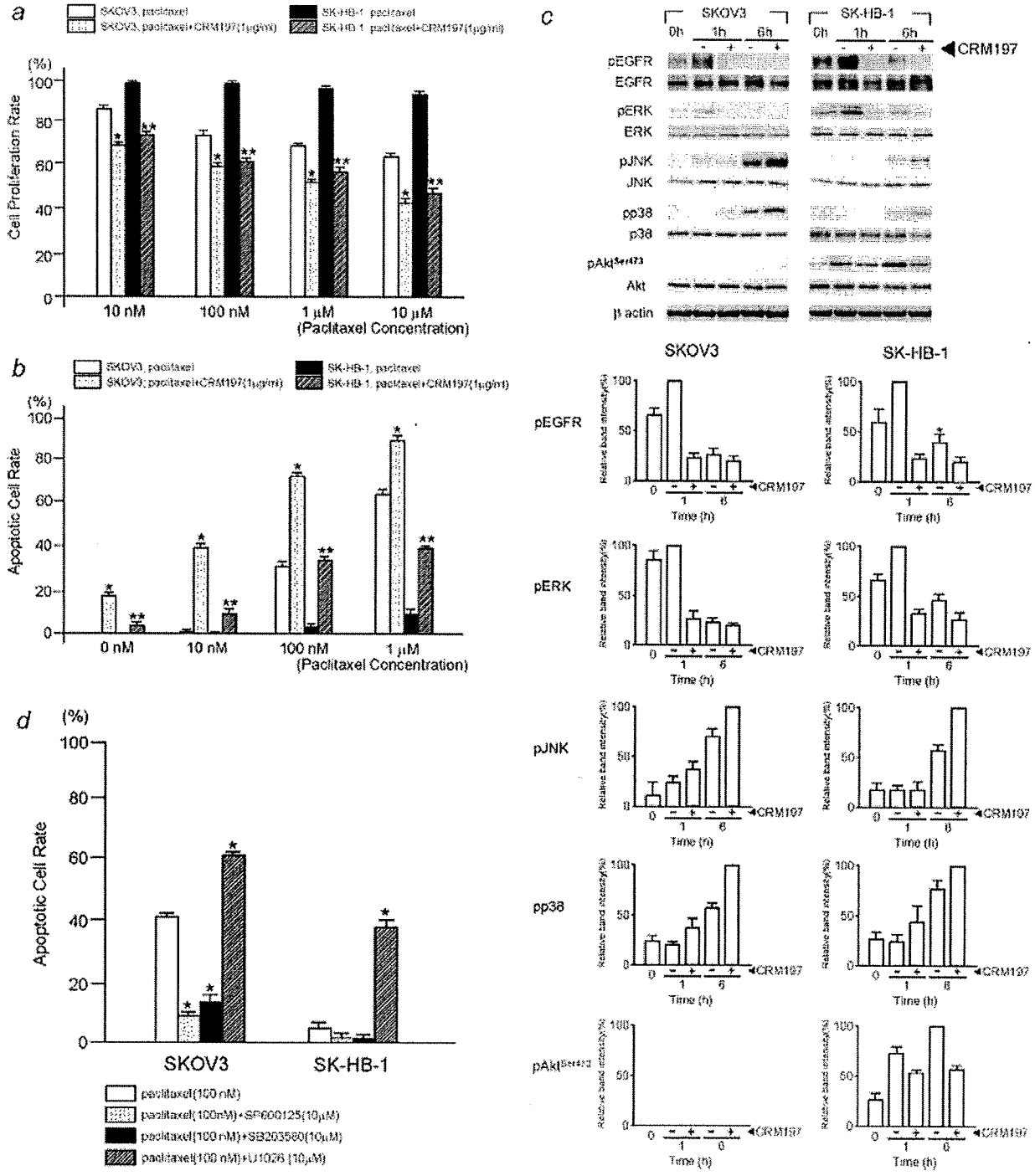

FIGURE 4 – CRM197 restores paclitaxel-mediated *in vitro* anti-tumor activity and MAPK signaling in SKOV3 and SK-HB-1 cells. SKOV3 and SK-HB-1 cells were incubated for 24 hr (*a*) or 48 hr (*b*) with various concentrations of paclitaxel in the presence or absence of 1 μg/ml CRM197. The values for cell proliferation rate (*a*) (paclitaxel: 10 nM–10 μM) or apoptotic cell rate (*b*) (paclitaxel: 10 nM–1 μM) were determined by MTT assay or by flow cytometric analysis. The values represent the means ± SD ($n = 4$). Statistical analysis was performed using the Mann-Whitney *U* test. *$p < 0.05$, *versus* the values for each concentration of paclitaxel in SKOV3 cells. **$p < 0.05$, *versus* the values for each concentration of paclitaxel in SK-HB-1 cells. SKOV3; open bars (paclitaxel) and dotted bars (paclitaxel plus CRM197), SK-HB-1; closed bars (paclitaxel) and hatched bars (paclitaxel plus CRM197). *C*. Alterations in MAPK signals. SKOV3 and SK-HB-1 cells were treated with 10 μM paclitaxel for the indicated length of time in the presence or absence of 1 μg/ml CRM197, and the activation statuses of EGFR, ERK, JNK, p38 and Akt were examined by immunoblotting and densitometric analysis. The values represent the mean ± SD ($n = 3$). The strongest band in each experiment is defined as 100 % of band intensity. (*d*) Cell apoptosis mediated by paclitaxel. SKOV3 and SK-HB-1 cells were treated with 100 nM of paclitaxel with or without SP600125 (10 μM), SB203580 (10 μM) or U0126 (10 μM) for 48 hr. The values for apoptotic cell rate were determined by flow cytometric analysis. The values represent the means ± SD ($n = 4$). Statistical analysis was performed using Tukey HSD test. *$p < 0.05$, *versus* the values for paclitaxel (100 nM) in SKOV3 or SK-HB-1 cells. Open bars (presence of paclitaxel), dotted bars (presence of paclitaxel plus SP600125), closed bars (presence of paclitaxel plus SB203580) and hatched bars (presence of paclitaxel plus U0126).

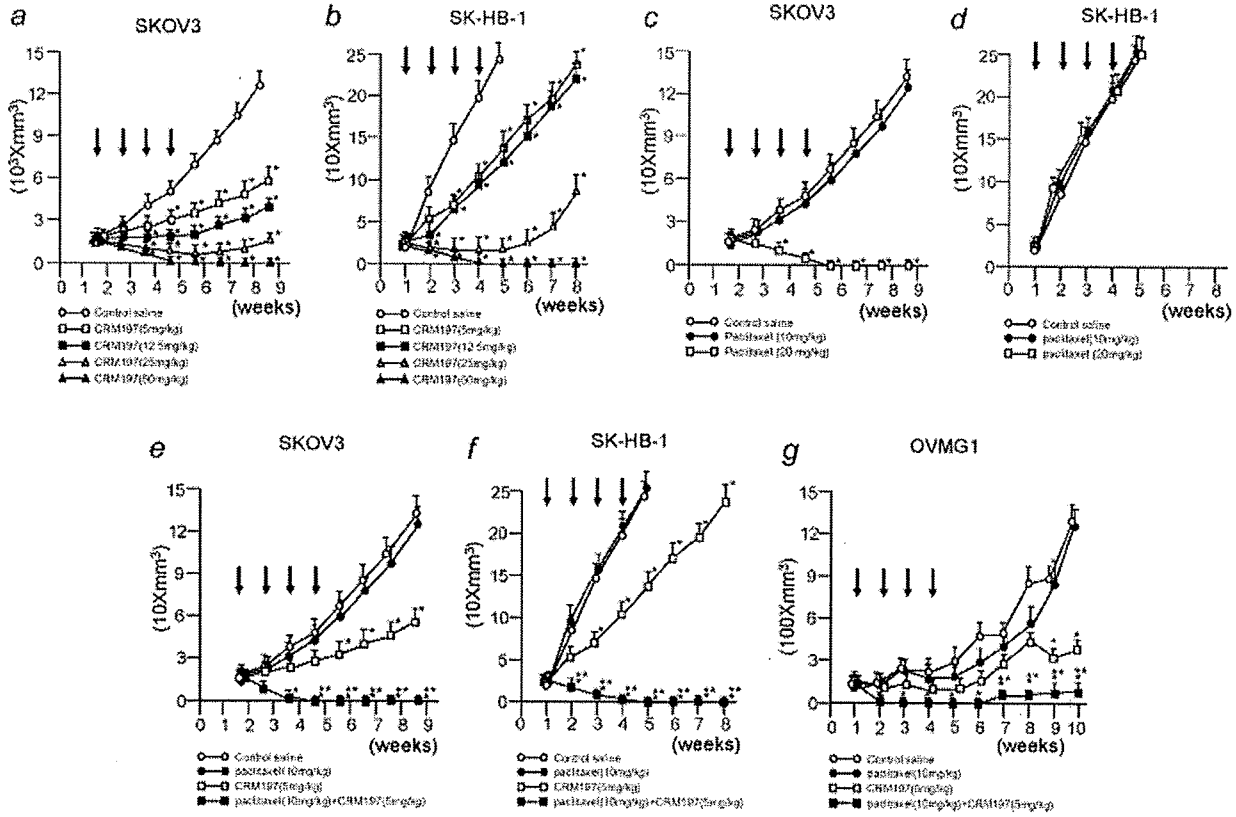

FIGURE 5 – Synergistic anti-tumor effect of CRM197 with paclitaxel. (*a*), (*b*) Dose-dependent suppression of tumor growth by SKOV3 (*a*) or SK-HB-1 (*b*) cells in nude mice by administration of CRM197. (*c*), (*d*) Dose-dependent suppression of tumor growth by SKOV3 (*c*) or SK-HB-1 (*d*) cells in nude mice by administration of paclitaxel. Ten or 7 days after injection of SKOV3 or SK-HB-1 cells, the indicated amount of CRM197 or control saline was injected intraperitoneally each week for 4 weeks. (*e*), (*f*), (*g*) Synergistic effect of paclitaxel and CRM197 on tumor growth by SKOV3 (*e*), SK-HB-1 (*f*) or OVMG1 (*g*) cells. Mice injected with SKOV3 or SK-HB-1 cells were administered with either paclitaxel alone (10 mg/kg), CRM197 alone (5 mg/kg) or both, each week for 4 weeks. Tumor volume was calculated as described in the "Materials and methods" section. Each tumor volume represents the mean ± SD ($n = 8$). Statistical analysis was performed using Tukey HSD test. $*p < 0.05$, *versus* the values for control mice injected with SKOV3 or SK-HB-1 cells. $**p < 0.05$, *versus* the values for mice, which were administered with CRM197 alone (5 mg/kg), injected with SKOV3 or SK-HB-1 cells.

These results indicate the existence of a synergistic *in vivo* anti-tumor effect induced by a combination of CRM197 with paclitaxel. These results suggest that a synergistic anti-tumor effect is provided by the combination of CRM197 with paclitaxel in ovarian cancer therapy.

Discussion

In this study, we showed that elevated expression of HB-EGF modulates the anti-tumor effect of paclitaxel, and that CRM197 restores this effect of paclitaxel. Moreover, we demonstrated that co-administration of paclitaxel and CRM197 synergistically suppressed tumor formation by ovarian cancer cells in mice. This synergistic effect could be explained by a change in the balance of anti-apoptotic activity and pro-apoptotic activity (Fig. 6).

Paclitaxel-induced apoptosis is associated with a stimulation of c-Raf-1 phosphorylation and activation of ERK.[30,31] The HB-EGF gene has been identified as an immediate-early transcriptional target of oncogenic Raf kinases and an early response gene to chemotherapy.[32,33] The shedding of proHB-EGF is regulated by the activation of Raf/ ERK kinase.[34,35] According to this evidence, the activation of Raf kinase by paclitaxel may result in the cleavage of HB-EGF, accompanied by the activation of ERK. However, in this study, ERK activation by paclitaxel occurred transiently, and neither ectodomain shedding of HB-EGF nor activation of ERK was observed over time. The enrichment of sHB-EGF in the culture medium sustained the cleavage of proHB-EGF after the addition of paclitaxel, resulting in resistance to paclitaxel in ovarian cancer cell lines. Therefore, the interruption of an autocrine loop involving HB-EGF may contribute to the reduction in tumor growth in patients with ovarian cancer. Recently, proHB-EGF generates HB-EGF, a soluble ligand of EGFR as well as carboxy-terminal fragments (HB-EGF-CTFs). The binding proteins of cytoplasmic tail of proHB-EGF, such as promyelocytic leukemia zinc finger (PLZF), B-cell leukemia 6 (Bcl6) and BAG-1, have been identified.[36–38] PLZF and Bcl6 function as transcriptional repressors to negatively regulate the cell cycle.[39–42] Internalized HB-EGF-CTFs blocks the activity of PLZF or Bcl6 through their association.[37,38] In addition, the interaction of BAG-1 with proHB-EGF leads to decreased cell adhesion, increased resistance to apoptosis, and rapid secretion of soluble of HB-EGF.[36] BAG-1 has been also reported to bind the cytoplasmic domain of the Raf-1 kinase, HGF receptor and several members of steroid hormone receptor superfamily.[43–46] These molecules bound to cytoplamic domain of HB-EGF may be involved in aggressive behaviors of ovarian cancer cells mediated by enhanced HB-EGF expression.

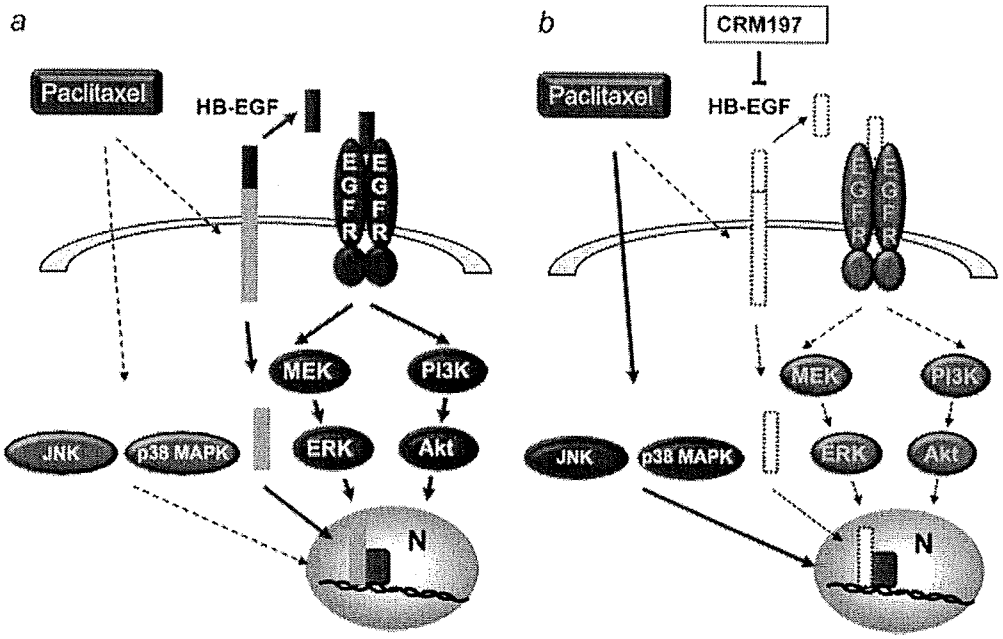

FIGURE 6 – Alterations in signalings treated with paclitaxel and/or CRM197. (*a*) Paclitaxel evokes the proapoptotic signals including JNK and p38 MAPK. Paclitaxel also promotes the ectodomain shedding of proHB-EGF, resulting in the activation of ERK and Akt as anti-apoptotic signals through EGFR transactivation. The carboxyl-terminal fragments of HB-EGF (HB-EGF-CTFs) go to nucleus to transmit the cell growth signal. Thus, the enhancement of HB-EGF expression possibly results in the acquisition of resistance to paclitaxel. (*b*) CRM197 blocks EGFR transactivation, leading to the suppression of ERK and Akt activation, and may inhibit the shift of HB-EGF-CTFs to nucleus. In the presence of CRM197, therefore, paclitaxel is hard to activate anti-apoptotic signals through the ectodomain shedding of HB-EGF. Paclitaxel may lend a strong impetus to proapoptotic signals. Accordingly, the combined treatment of paclitaxel with CRM197 induces synergistic anti-tumor effects in ovarian cancer. EGFR: epidermal growth factor receptor, HB-EGF: heparin binding-EGF like growth factor, MEK: mitogen activated protein kinase kinase, ERK: extracellular related protein kinase, PI3K: phosphatidylinositol 3-kinase, Akt: protein kinase B, JNK: Jun kinase, p38 MAPK: p38 mitogen activated protein kinase, N: nucleus, CRM197: cross-reacting material 197. Red circles: the activated forms of signaling molecules. Black circles: the inactivated forms of signaling molecules.

ERK and Akt can transmit anti-apoptotic signals into cells by activating BAD (Bcl-2-associated death protein), which can antagonize anti-apoptotic activity, forming heterodimers with the anti-apoptotic proteins Bcl-X_L or Bcl-2.[47,48] The two cascades of ERK and Akt, which have been identified as downstream components of survival signaling through EGFR, are implicated in resistance to anti-tumor agents.[49,50] The activation of Akt also suppresses the activity of apoptosis signal-regulating kinase 1 (ASK1), resulting in inhibition of JNK and p38 MAPK activation.[51,52] Therefore, CRM197 suppresses anti-apoptotic signals including ERK as well as Akt *via* the inhibition of HB-EGF function, and activates pro-apoptotic signals including JNK and p38 MAPK *via* the inhibition of Akt activity. Cisplatin and paclitaxel are available for the treatment of epithelial cancers.[53] Cisplatin is also implicated in the activation of members of the MAPK family, including ERK, JNK and p38 MAPK.[54] Cisplatin-mediated DNA damage induces the phosphorylation of both BAD Ser112 *via* an ERK cascade and BAD Ser136 *via* a PI3K-Akt cascade, and inhibition of either of these cascades sensitizes ovarian cancer cells to cisplatin.[55] Many other anti-tumor agents can also activate members of the MAPK family, although the kinetics of activation is different. With increased evidence supporting a role for MAPK signaling in anti-tumor drug action, MAPK modulators may have potential as chemotherapeutic drugs themselves or as chemosensitizing agents.[4] Up to date, it has been reported that the antibodies against ERGF or HER2 can potentiate the DNA-damaging cytotoxic effects of chemotherapeutic agents.[56,57] CRM197 may enhance the same DNA-damaging cytotoxic anti-tumor effects of paclitaxel as anti-EGFR antibodies (Fig. 6). Since elucidation of some of the molecular mechanisms of EGFR-mediated chemoresistance leads to novel approaches against molecules linked to EGFR signal transduction, recent clinical trials, which have been designed to combine EGFR inhibitors with standard chemotherapies, have been successful.[58] Additionally, PLZF, Bcl6 and BAG1 bound to cytoplasmic domain of HB-EGF regulate cell behavior[36–38] and the blockage of ectodomain shedding of HB-EGF inhibits cell growth through the inhibition of HB-EGF-CTF nuclear translocation.[59] It is, therefore, plausible that CRM197 stimulates the function of PLZF or Bcl6 and suppresses the activity of BAG-1 *via* a decrease of HB-EGF-CTFs. These binding proteins of HB-EGF-CTFs may also facilitate to enhance the anti-tumor effects of paclitaxel and CRM197 (Fig. 6).

A clinical trial of CRM197 was performed in 25 patients with advanced human cancer.[60] In this trial, 2 patients indicated a complete response, 1 patient showed a partial response, and 6 patients showed stable disease. This study also reported that toxicities were minimal, since only 1 patient had irritating skin reactions in the injection sites and a flu-like syndrome with fever, suggesting that CRM197 can be recognized as a useful safety agent for cancer therapy. Phase 1 study of the use of CRM197 has been already started for patients with advanced ovarian cancer in Fukuoka University under the approval of the ethical committee. In this study, the enhancement of HB-EGF expression abrogates the anti-tumor effect of paclitaxel by altering the balance of anti-apoptotic and pro-apoptotic signals induced by paclitaxel. The treatment of CRM197 in conjunction with paclitaxel results in a marked synergistic anti-tumor effect in ovarian cancer cells *in vivo*, suggesting a novel combination therapy for ovarian cancer patients including those showing chemo-resistance.

Acknowledgements

This work was supported in part by a Grant-in-aid for Scientific Research on Priority Areas, Fukuoka University Research Foundation and Research Promotion for Innovative Therapies against Cancers from the Ministry of Education, Culture, Sports, Science and Technology to E.M.

References

1. Schiff PB, Fant J, Horwitz SB. Promotion of microtubule assembly *in vitro* by taxol. Nature 1979;277:665–7.
2. Sarosy G, Reed E. Taxol dose intensification and its clinical implications. J Natl Med Assoc 1993;85:427–31.
3. Rowinsky EK. Update on the antitumor activity of paclitaxel in clinical trials. Ann Pharmacother 1994;28(5 Suppl):S18–S22.
4. Fan M, Chambers TC. Role of mitogen-activated protein kinases in the response of tumor cells to chemotherapy. Drug Resist Update 2001;4:253–67.
5. Okano J, Rustgi AK. Paclitaxel induces prolonged activation of the Ras/MEK/ERK pathway independently of activating the programmed cell death machinery. J Biol Chem 2001;276:19555–64.
6. Riese DJ, II, Stern DF. Specificity within the EGF family/ErbB receptor family signaling network. Bioessays 1998;20:41–8.
7. Higashiyama S, Abraham JA, Miller J, Fiddes JC, Klagsbrun M. A heparin-binding growth factor secreted by macrophage-like cells that is related to EGF. Science 1991;251:936–9.
8. Izumi Y, Hirata M, Hasuwa H, Iwamoto R, Umata T, Miyado K, Tamai Y, Kurisaki T, Sehara-Fujisawa A, Ohno S, Mekada E. A metalloprotease-disintegrin MDC9/meltrin-gamma/ADAM9 and PKCdelta are involved in TPA-induced ectodomain shedding of membrane-anchored heparin-binding EGF-like growth factor. EMBO J 1998;17:7260–72.
9. Seals DF, Courtneidge SA. The ADAMs family of metalloproteases: multidomain proteins with multiple functions. Genes Dev 2003;17:7–30.
10. Prenzel N, Zwick E, Daub H, Leserer M, Abraham R, Wallasch C, Ullrich A. EGF receptor transactivation by G-protein-coupled receptors requires metalloproteinase cleavage of proHB-EGF. Nature 1999; 402:884–8.
11. Takenobu H, Yamazaki A, Hirata M, Umata T, Mekada E. The stress- and inflammatory cytokine-induced ectodomain shedding of heparin-binding epidermal growth factor-like growth factor is mediated by p38 MAPK, distinct from the 12-O-tetradecanoylphorbol-13-acetate- and lysophosphatidic acid-induced signaling cascades. J Biol Chem 2003;278:17255–62.
12. Goishi K, Higashiyama S, Klagsbrun M, Nakano N, Umata T, Ishikawa M, Mekada E, Taniguchi N. Phorbol ester induces the rapid processing of cell surface heparin-binding EGF-like growth factor: conversion from juxtacrine to paracrine growth factor activity. Mol Biol Cell 1995;6:967–80.
13. Dethlefsen SM, Raab G, Moses MA, Adam RM, Klagsbrun M, Freeman MR. Extracellular calcium influx stimulates metalloproteinase cleavage and secretion of heparin-binding EGF-like growth factor independently of protein kinase C. J Cell Biochem 1998; 69:143–53.
14. Tanida S, Joh T, Itoh K, Kataoka H, Sasaki M, Ohara H, Nakazawa T, Nomura T, Kinugasa Y, Ohmoto H, Ishiguro H, Yoshino K, et al. The mechanism of cleavage of EGFR ligands induced by inflammatory cytokines in gastric cancer cells. Gastroenterology 2004;127:559–69.
15. Gechtman Z, Alonso JL, Raab G, Ingber DE, Klagsbrun M. The shedding of membrane-anchored heparin-binding epidermal-like growth factor is regulated by the Raf/mitogen-activated protein kinase cascade and by cell adhesion and spreading. J Biol Chem 1999;274: 28828–35.
16. Iwamoto R, Mekada E. Heparin-binding EGF-like growth factor: a juxtacrine growth factor. Cytokine Growth Factor Rev 2000;11:335–44.
17. Nanba D, Higashiyama S. Dual intracellular signaling by proteolytic cleavage of membrane-anchored heparin-binding EGF-like growth factor. Cytokine Growth Factor Rev 2004;15:13–9.
18. Nishi E, Klagsbrun M. Heparin-binding epidermal growth factor-like growth factor (HB-EGF) is a mediator of multiple physiological and pathological pathways. Growth Factors 2004;22:253–60.
19. Miyamoto S, Yagi H, Yotsumoto F, Kawarabayashi T, Mekada E. Heparin-binding epidermal growth factor-like growth factor as a novel targeting molecule for cancer therapy. Cancer Sci 2006;97: 341–7.
20. Miyamoto S, Hirata M, Yamazaki A, Kageyama T, Hasuwa H, Mizushima H, Tanaka Y, Yagi H, Sonoda K, Kai M, Kanoh H, Nakano H, et al. Heparin-binding EGF-like growth factor is a promising target for ovarian cancer therapy. Cancer Res 2004;64:5720–7.
21. Yagi H, Miyamoto S, Tanaka Y, Sonoda K, Kobayashi H, Kishikawa T, Iwamoto R, Mekada E, Nakano H. Clinical significance of heparin-binding epidermal growth factor-like growth factor in peritoneal fluid of ovarian cancer. Br J Cancer 2005;92:1737–45.
22. Mitamura T, Higashiyama S, Taniguchi N, Klagsbrun M, Mekada E. Diphtheria toxin binds to the epidermal growth factor (EGF)-like domain of human heparin-binding EGF-like growth factor/diphtheria toxin receptor and inhibits specifically its mitogenic activity. J Biol Chem 1995;270:1015–9.
23. Tanaka Y, Miyamoto S, Suzuki SO, Oki E, Yagi H, Sonoda K, Yamazaki A, Mizushima H, Maehara Y, Mekada E, Nakano H. Clinical significance of heparin-binding epidermal growth factor-like growth factor and a disintegrin and metalloprotease 17 expression in human ovarian cancer. Clin Cancer Res 2005;11: 4783–92.
24. Uchida T, Pappenheimer AM, Jr, Greany R. Diphtheria toxin and related proteins. I. Isolation and properties of mutant proteins serologically related to diphtheria toxin. J Biol Chem 1973;248:3838–44.
25. Yamazaki S, Iwamoto R, Saeki K, Asakura M, Takashima S, Yamazaki A, Kimura R, Mizushima H, Moribe H, Higashiyama S, Endoh M, Kaneda Y, et al. Mice with defects in HB-EGF ectodomain shedding show severe developmental abnormalities. J Cell Biol 2003; 163:469–75.
26. Hasuwa H, Kaseda K, Einarsdottir T, Okabe M. Small interfering RNA and gene silencing in transgenic mice and rats. FEBS Lett 2002; 532:227–30.
27. Okugawa K, Kobayashi H, Hirakawa T, Sonoda T, Ogura T, Nakano H. *In vivo* establishment and characterization of a paclitaxel-resistant human ovarian cancer cell line showing enhanced growth properties and drug-resistance only *in vivo*. J Cancer Res Clin Oncol 2004; 130:178–86.
28. Iwamoto R, Higashiyama S, Mitamura T, Taniguchi N, Klagsbrun M, Mekada E. Heparin-binding EGF-like growth factor, which acts as the diphtheria toxin receptor, forms a complex with membrane protein DRAP27/CD9, which up-regulates functional receptors and diphtheria toxin sensitivity. EMBO J 1994;13:2322–30.
29. Higashiyama S, Iwamoto R, Goishi K, Raab G, Taniguchi N, Klagsbrun M, Mekada E. The membrane protein CD9/DRAP27 potentiates the juxtacrine growth factor actiovity of the membrane-anchored heparin-binding EGF-like growth factor. J Cell Biol 1995;128:929–38.
30. Blagosklonny MV, Schulte TW, Nguyen P, Mimnaugh EG, Trepel J, Neckers L. Taxol induction of p21WAF1 and p53 requires c-raf-1. Cancer Res 1995;55:4623–6.
31. Blagosklonny MV, Schulte T, Nguyen P, Trepel J, Neckers LM. Taxol-induced apoptosis and phosphorylation of Bcl-2 protein involves c-Raf-1 and represents a novel c-Raf-1 signal transduction pathway. Cancer Res 1996;56:1851–4.
32. McCarthy SA, Samuels ML, Pritchard CA, Abraham JA, McMahon M. Rapid induction of heparin-binding epidermal growth factor/diphtheria toxin receptor expression by Raf and Ras oncogenes. Genes Dev 1995;9:1953–64.
33. Wang F, Liu R, Lee SW, Sloss CM, Couget J, Cusack JC. Heparin-binding EGF-like growth factor is an early response gene to chemotherapy and contributes to chemotherapy resistance. Oncogene 2007; 26:2006–16.
34. Goechtman Z, Alonso JL, Raab G, Ingber DE, Klagsbrun M. The shedding of membrane-anchored heparin-binding epidermal-like growth factor is regulated by the Raf/mitogen-activated protein kinase cascade and by cell adhesion and spreading. J Biol Chem 1999; 274:28828–35.
35. Umata T, Hirata M, Takahashi T, Ryu F, Shida S, Takahashi Y, Tsuneoka M, Miura Y, Masuda M, Horiguchi Y, Mekada E. A dual signaling cascade that regulates the ectodomain shedding of heparin-binding epidermal growth factor-like growth factor. J Biol Chem 2001;276:30475–82.
36. Lin J, Hutchinson L, Gaston SM, Raab G, Freeman MR. BAG-1 is a novel cytoplasmic binding partner of the membrane form of heparin-binding EGF-like growth factor: a unique role for proHB-EGF in cell survival regulation. J Biol Chem 201;267:30127–32.
37. Nanba D, Mammoto A, Hashimoto K, Higashiyama S. Proteolytic release of the carboxy-terminal fragment of proHB-EGF causes nuclear export of PLZF. J Cell Biol 2003;163:489–502.
38. Kinugasa Y, Hieda M, Hori M, Higashiyama S. The carboxyl-terminal fragment of pro-HB-EGF reverses Bcl6-mediated gene repression. J Biol Chem 2007;282:14797–806.
39. Yeyati PL, Shaknovich R, Boterashvili S, Li J, Ball HJ, Waxman S, Nason-Burchenal K, Dmitrovsky E, Zelent A, Licht JD. Leukemia translocation protein PLZF inhibits cell growth and expression of cyclin A. Oncogene 1999;18:925–34.

40. McConnell MJ, Chevallier N, Berkofsky-Fessler W, Giltnane JM, Malani RB, Staudt LM, Licht JD. Growth suppression by acute promyelocytic leukemia-associated protein PLZF is mediated by repression of c-myc expression. Mol Cell Biol 2003;23:9375–88.
41. Fernández de Mattos S, Essafi A, Soeiro I, Pietersen AM, Birkenkamp KU, Edwards CS, Martino A, Nelson BH, Francis JM, Jones MC, Brosens JJ, Coffer PJ, et al. FoxO3a and BCR-ABL regulate cyclin D2 transcription through a STAT5/BCL6-dependent mechanism. Mol Cell Biol 2004;24:10058–71.
42. Chattopadhyay A, Tate SA, Beswick RW, Wagner SD, Ko Ferrigno P. A peptide aptamer to antagonize BCL-6 function. Oncogene 2006; 25:2223–33.
43. Bardelli A, Longati P, Albero D, Goruppi S, Schneider C, Ponzetto C, Comoglio PM. HGF receptor associates with the anti-apoptotic protein BAG-1 and prevents cell death. EMBO J 1996;15:6205–12.
44. Froesch BA, Takayama S, Reed JC. BAG-1L protein enhances androgen receptor function. J Biol Chem 1998;273:11660–6.
45. Wang HG, Takayama S, Rapp UR, Reed JC. Bcl-2 interacting protein BAG-1, binds to and activates the kinase. Raf-1. Proc Natl Acad Sci USA 1996;93:7063–8.
46. Schneikert J, Hübner S, Martin E, Cato AC. A nuclear action of the eukaryotic cochaperone RAP46 in downregulation of glucocorticoid receptor activity. J Cell Biol 1999;146:929–40.
47. Datta SR, Ranger AM, Lin MZ, Sturgill JF, Ma YC, Cowan CW, Dikkes P, Korsmeyer SJ, Greenberg ME. Survival factor-mediated BAD phosphorylation raises the mitochondrial threshold for apoptosis. Dev Cell 2002;3:631–43.
48. Mabuchi S, Ohmichi M, Kimura A, Hisamoto K, Hayakawa J, Nishio Y, Adachi K, Takahashi K, Arimoto-Ishida E, Nakatsuji Y, Tasaka K, Murata Y. Inhibition of phosphorylation of BAD and Raf-1 by Akt sensitizes human ovarian cancer cells to paclitaxel. J Biol Chem 2002;277:33490–500.
49. Yang JY, Michod D, Walicki J, Widmann C. Surviving the kiss of death. Biochem Pharmacol 2004;68:1027–31.
50. Ohmichi M, Hayakawa J, Tasaka K, Kurachi H, Murata Y. Mechanisms of platinum drug resistance. Trends Pharmacol Sci 2005;26: 113–6.
51. Kim AH, Khursigara G, Sun X, Franke TF, Chao MV. Akt phosphorylates and negatively regulates apoptosis signal-regulating kinase 1. Mol Cell Biol 2001;21:893–901.
52. Park HS, Kim MS, Huh SH, Park J, Chung J, Kang SS, Choi EJ. Akt (protein kinase B) negatively regulates SEK1 by means of protein phosphorylation. J Biol Chem 2002;277:2573–8.
53. Ozols RF, Bookman MA, Connolly DC, Daly MB, Godwin AK, Schilder RJ, Xu X, Hamilton TC. Focus on epithelial ovarian cancer. Cancer Cell 2004;5:19–24.
54. Siddik ZH. Cysplatin: mode of cytotoxic action and molecular basis of resistance. Oncogene 2003;22:7265–79.
55. Hayakawa J, Ohmichi M, Kurachi H, Kanda Y, Hisamoto K, Nishio Y, Adachi K, Tasaka K, Kanzaki T, Murata Y. Inhibition of BAD phosphorylation either at serine 112 *via* extracellular signal-regulated protein kinase cascade or at serine 136 *via* Akt cascade sensitizes human ovarian cancer cells to cisplatin. Cancer Res 2000;60:5988–94.
56. Lopez AM, Pegram MD, Slamon DJ, Landaw EM. A model-based approach for assessing *in vivo* combination therapy interactions. Proc Natl Acad Sci USA 1999;96:13023–8.
57. Pegram MD, Konecny GE, O'Callaghan C, Beryt M, Pietras R, Slamon DJ. Rational combinations of trastuzumab with chemotherapeutic drugs used in the treatment of breast cancer. J Natl Cancer Inst 2004;96:739–49.
58. Schmidt M, Lichtner RB. EGF receptor targeting in therapy-resistant human tumors. Drug Resist Update 2002;5:11–18.
59. Shimura T, Kataoka H, Ogasawara N, Kubota E, Sasaki M, Tanida S, Joh T. Suppression of proHB-EGF carboxy-terminal fragment nuclear translocation: a new molecular target therapy for gastric cancer. Clin Cancer Res 2008;14:3956–65.
60. Buzzi S, Rubboli D, Buzzi G, Buzzi AM, Morisi C, Pironi F. CRM197 (nontoxic diphtheria toxin): effects on advanced cancer patients. Cancer Immunol Immunother 2004;53:1041–8.

Cardiovascular Research (2009) 81, 457–464
doi:10.1093/cvr/cvn335

Review

Oxidative stress and left ventricular remodelling after myocardial infarction

Masatsugu Hori[1]* and Kazuhiko Nishida[2]

[1]*Osaka Medical Center for Cancer and Cardiovascular Diseases, 1-3-3 Nakamichi, Higashinari-ku, Osaka 537-8511, Japan; and* [2]*Department of Cardiovascular Medicine, Osaka University Graduate School of Medicine, 2-2 Yamadaoka, Suita 565-0871, Osaka, Japan*

Received 27 August 2008; revised 5 November 2008; accepted 27 November 2008; online publish-ahead-of-print 1 December 2008

Time for primary review: 24 days

KEYWORDS
Oxidative stress;
Reactive oxygen species;
Inflammatory cytokine;
Remodelling;
Myocardial infarction

In acute myocardial infarction (MI), reactive oxygen species (ROS) are generated in the ischaemic myocardium especially after reperfusion. ROS directly injure the cell membrane and cause cell death. However, ROS also stimulate signal transduction to elaborate inflammatory cytokines, e.g. tumour necrosis factor-α (TNF-α), interleukin (IL)-1β and -6, in the ischaemic region and surrounding myocardium as a host reaction. Inflammatory cytokines also regulate cell survival and cell death in the chain reaction with ROS. Both ROS and inflammatory cytokines are cardiodepressant mainly due to impairment of intracellular Ca^{2+} homeostasis. Inflammatory cytokines stimulate apoptosis through a TNF-α receptor/caspase pathway, whereas Ca^{2+} overload induced by extensive ROS generation causes necrosis through enhanced permeability of the mitochondrial membrane (mitochondrial permeability transition). Apoptosis signal-regulating kinase-1 (ASK1) is an ROS-sensitive, mitogen-activated protein kinase kinase kinase that is activated by many stress signals and can activate nuclear factor κB and other transcription factors. ASK1-deficient mice demonstrate that the ROS/ASK1 pathway is involved in necrotic as well as apoptotic cell death, indicating that ASK1 may be a therapeutic target to reduce left ventricular (LV) remodelling after MI. ROS and inflammatory cytokines activate matrix metalloproteinases which degrade extracellular matrix, causing a slippage of myofibrils and hence LV dilatation. Consequently, collagen deposition is increased and tissue repair is enhanced with myocardial fibrosis and angiogenesis. Since the extent of LV remodelling is a major predictor of prognosis of the patients with MI, the therapeutic approach to attenuating LV remodelling is critically important.

1. Introduction

The most important structural event after myocardial infarction (MI) is left ventricular (LV) remodelling.[1,2] Remodelling of the heart is derived from intra- and extracellular structural changes of the myocardium and elicits structural changes of the LV wall. Further mechanical load on the LV wall causes LV dilatation. Thus, the extent of LV remodelling could be a predictive factor for mortality and morbidity of the patient with MI.[3]

The underlying mechanism of LV remodelling is multifactorial; many biological reactions are involved in the time course of remodelling after an ischaemic episode: (i) local ischaemia and myocardial cell death, (ii) oxidative stress and inflammatory reactions in injured myocardium,[4] (iii) cardiodepressive reactions due to the production of reactive oxygen species (ROS) and inflammatory cytokines,[5,6] (iv) changes in extracellular matrix following activations of matrix metalloproteinases (MMPs),[7,8] (v) structural changes of myocardium in response to mechanical stress, and (vi) synthesis of collagens and myocardial fibrosis.[9] These reactive processes are related each other and proceed from acute reactions to chronic changes. LV remodelling ultimately elicits LV dilatation usually with LV dysfunction and thus could be one of the most important determinant of prognosis of the patients with MI.

MI is usually initiated by myocardial ischaemia due to coronary artery obstruction. In the ischaemic myocardium, ROS are generated, especially after reperfusion.[10,11] The major sources of ROS in the ischaemic-reperfused myocardium are mitochondria, xanthine oxidase, and phagocyte nicotinamide adenine dinucleotide phosphate (NADPH) oxidase.[12–14] ROS directly injure the tissue as key molecules for inducing cell death. Detrimental effects of ROS are clearly demonstrated by the findings that in the transgenic mice in which an antioxidant protein, superoxide dismutase (SOD) is overexpressed, infarct size is markedly reduced.[15,16]

In the ischaemic region and surrounding myocardium, inflammatory cytokines, e.g. tumour necrosis factor-α

* Corresponding author. Tel: +81 6 6972 1181; fax: +81 6 6981 7050.
E-mail address: hori-ma@mc.pref.osaka.jp

(TNF-α), IL-1β, and IL-6 are produced as a host reaction.[17] The inflammatory cytokines regulate cell survival and cell death, and could be a trigger of another inflammatory reaction.[18] ROS stimulate the production of inflammatory cytokines and inversely, inflammatory cytokines stimulate ROS formation.[19] In chronic stage, ROS and inflammatory cytokines activate the MMPs and collagen deposit which contribute to the structural changes and tissue repair of injured myocardium.[20,21] Activations of MMPs elicit degradation of collagens which may cause a slippage in myofibrillar alignment causing LV dilatation.[22] During tissue repair, the cytokines activate angiogenesis and mobilization of stem cells and hereby contribute to late remodelling.

2. Cardiodepression and remodelling through oxidative stress and inflammatory cytokines

Myocardial ischaemia either with or without reperfusion induces ROS and inflammatory cytokines. It is of note that these reactive molecules are cardiodepressant through impairment of Ca^{2+} homeostasis. ROS can induce intracellular Ca^{2+} overload during oxidative stress.[12,23] ROS cause extracellular Ca^{2+} influx mediated by increased membrane lipid peroxidation and the opening of voltage-sensitive Ca^{2+} channels or Na^{+}/Ca^{2+} exchanger.[24] ROS also cause a release of Ca^{2+} from intracellular stores and attenuate Ca^{2+} uptake by sarcoplasmic reticulum Ca^{2+}ATPase.[24]

Inflammatory cytokines, e.g. TNF-α and IL-6 also cause dysregulation of intracellular Ca^{2+}; TNF-α decreases Ca^{2+} sensitivity of myofibrils through nitric oxide as well as neutral sphingomyelinase; sustained induction of TNF-α inhibits expression of SERCA2a and elicits persistent depression of Ca^{2+} pump of sarcoplasmic reticulum.[25] These detrimental effects of inflammatory cytokines could be partially inhibited by radical scavengers indicating that detrimental effects of the inflammatory cytokines are partially mediated with ROS.[26]

After MI, MMPs and tissue inhibitors of MMPs (TIMPs) play an important role in cardiac repair and LV remodelling. A key process in LV enlargement is activation of MMPs in the extracelluar matrix;[27] collagenases (MMP-1, -8, and -13), gelatinases (MMP-2 and -9), stromelysins (MMP-3, -10, and -11), and membrane-type MMPs. TIMPs regulate MMP activities by their inhibiting actions. Thus, degradation of collagen is regulated by the balance of these competitive protein activities. It is also reported that inflammatory cytokines and ROS mediate MMP induction or stimulation and decrease TIMP levels and collagen synthesis;[8] structural changes of myocardial tissue are elaborated by sustained induction of inflammatory cytokines.

In transgenic mice with cardiac overexpression of TNF-α, the heart is enlarged and dilated with marked inflammatory cell infiltration and myocardial fibrosis.[28,29] In this transgenic mice, MMP activations are observed by gelatin zymography.[29] TNF-α blocking protein prevents MMPs induction and myocardial remodelling in the dog pacing-induced heart failure (HF) model, suggesting that TNF-α blocking protein prevents the local induction of MMPs.[30] In transgenic mice with cardiac overexpression of TNF-α, it is also reported that further collagen synthesis, deposition and denaturation are prevented and LV diastolic function is improved, when MMP-2 and MMP-9 expressions are attenuated by inhibition of TNF-α with adenovirus infection expressing soluble TNF-α receptor type I, suggesting that the extracellular matrix changes regulate diastolic function of the heart.[31] In an *in vivo* mouse model of MI, a hydroxyl radical scavenger attenuates the increased myocardial MMP-2 activity and LV remodelling.[32] A clinical study has also demonstrated a positive correlation between a specific marker of oxidative stress and relative level of MMP-2 and MMP-9 in patients with coronary artery disease.[33] These reports strongly suggest that oxidative stress plays an important role in MMP regulation and hence, LV remodelling.

Indeed, the activated MMPs degrade the extracellular matrix, disrupting the fibrillar collagen network and allowing inflammatory cells to migrate into the infarct tissue to remove necrotic myocytes.[34] In the mouse MI model, MMP-9 is mainly expressed in infiltrating neutrophils and macrophages of the infarcted area. Subsequently, MMP-9 activity further increases. Thereafter, MMP-2 activity starts to increase, whereas MMP-9 gradually decreases. During early remodelling phase, the necrotic tissue in infarcted area is replaced by granulation tissue with a collagen-rich matrix. In the remote area, cytokines are activated if the infarct size is large, or if there are other ongoing myocardial stress factors. Also, during late remodelling phase, MMPs and TIMPs continue to play an important role in the remodelling process in the infarcted and remote areas.[34]

3. Reactive oxygen species as intracellular signalling molecules

ROS are major initiators of myocardial damage during ischaemia/reperfusion.[13] It is reported that the development of infarction following myocardial ischaemia/reperfusion is associated with the population of apoptotic cells in peri-necrotic area.[35] Treatments with antioxidant agents or upregulation of endogenous antioxidant enzymes could protect against reperfusion injury.[36–38] Neutrophils are the primary source of ROS during reperfusion.[13] Endothelial cells and cardiomyocytes can also generate ROS. ROS are produced from xanthine oxidase in endothelial cells, mitochondrial electron transport chain reactions in cardiomyocytes, and NADPH oxidase in inflammatory cells.[12–14] A burst of ROS from endothelial cells and cardiomyocytes can amplify local inflammatory response and influence nearby neutrophils, leading to a chain reaction of ROS generation.[39]

In contrast to the direct actions of ROS on cellular injury, ROS play an important role in cell protection as intracellular signalling molecules mediated by the activation and expression of antioxidant enzymes. The low-level oxidant production may be a trigger for ischaemic preconditioning.[40] The delayed pre-conditioning is also tightly related to the production of ROS and the synthesis of antioxidant enzyme, manganese-SOD, after initial ischaemic stress.[41] ROS can activate an ROS-sensitive mitogen-activated protein (MAP) kinase kinase kinase, apoptosis signal-regulating kinase 1 (ASK1), which activates the downstream MAP kinases, p38, and c-Jun N-terminal kinase (JNK).[42] ROS activate nuclear factor κB (NF-κB) mediated through ASK1.[43] The activation of NF-κB can produce TNF-α, leading to activation of extrinsic apoptotic pathway mediated by death receptors[44] as well as activation

of hypertrophic response.[45] It is of interest that TNF-α can also generate ROS which can further activate NF-κB.[45] ROS also stimulate other transcription factors such as Ets and activator protein-1 (AP-1) mediated through Akt and protein kinase C pathways.[46] Oxidative stress-induced activation of transcription factors leads to synthesis of antioxidant enzymes such as manganese-SOD and endothelial nitric-oxide synthase.[47] Thus, ROS are key players for cell protection as well as cell injury in response to oxidative stress.

4. Molecular mechanism of cardiomyocyte death mediated by oxidative stress and inflammatory cytokines

Oxidative stress and cytokines play a key role in both apoptotic and necrotic cardiomyocyte death. In apoptotic cardiomyocyte death, there are two major apoptotic signalling pathways i.e. intrinsic pathway via mitochondria and extrinsic pathway via Fas ligand or TNF-α.[44] In the intrinsic pathway, the pro-apoptotic Bcl-2 family e.g. Bax and Bak enhances the permeability of the mitochondrial outer membrane, leading to protein release such as cytochrome c from the intermembrane space to the cytoplasm (*Figure 1*).[48] In contrast, the extrinsic pathway is activated when death ligands, e.g. Fas ligand or TNF-α, bind to cognate receptors on the plasma membrane.[49] These receptors contain an intracellular death domain, which can recruit and activate caspase 8 via adaptor FADD (Fas-associated protein with the death domain), inducing cell death.[50,51]

Necrosis is classically characterized by early plasma membrane rupture and swelling of cytoplasmic organelles, in particular mitochondria.[52,53] Necrosis is often defined in a negative manner, as cell death lacking the characteristics of programmed cell death and thus accidental and uncontrolled.[54] Mitochondrial permeability transition (MPT), also known as mitochondrial depolarization, is defined as the loss of transmembrane potential of the mitochondrial inner membrane and is a Ca^{2+}-dependent increase in the permeability of the mitochondrial membrane, causing the loss of the proton gradient and the shutdown of ATP generation through oxidative phosphorylation (*Figure 1*). Consequently, this results in mitochondrial swelling and rupture of the outer membrane.[55,56] MPT is thought to occur after opening of a putative channel complex termed 'permeability transition pore' composed of the voltage-dependent anion channel, adenine nucleotide translocator, cyclophilin D (CypD), and other molecules.[57,58] MPT pores open in the mitochondrial inner membrane in response to stimuli such as increased intracellular Ca^{2+}, inorganic phosphate, alkaline pH, and ROS. Although the MPT pathway may induce apoptotic cell death under some condition, the MPT pore opening is recognized to be a major cause of the necrotic cell death.[59] CypD-deficient mice show a high level of resistance to ischaemia/reperfusion-induced cardiac necrosis,[60] indicating that ROS is involved in necrotic cardiomyocyte death through MPT pore opening. Thus, ROS could cause both apoptosis and necrosis although precise regulating mechanisms are not elucidated yet.

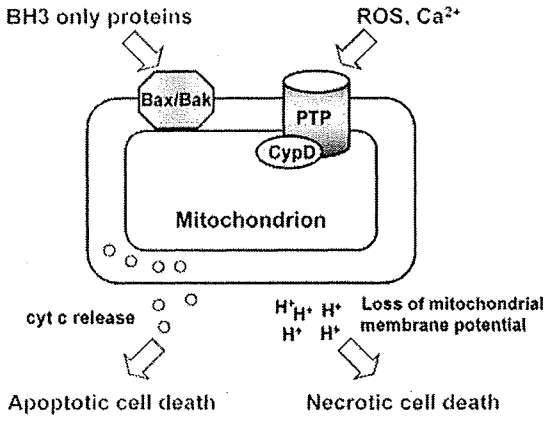

Figure 1 The mechanisms of apoptotic or necrotic cell death mediated through mitochondria. In intrinsic pathway of apoptosis, BH3-only proteins are activated by apoptotic stimuli. Active BH3-only proteins activate Bax and Bak. Once activated, Bax and Bak promote cytochrome c (cyt c) release from the intermembrane space to the cytoplasm, leading to apoptotic cell death. In contrast, Ca^{2+} overload induced by extensive ROS generation could enhance the permeability of the mitochondrial membrane mediated through opening of a putative channel complex, permeability transition pore (PTP), and lead to MPT, which is defined as the loss of transmembrane potential of the mitochondrial inner membrane, and then necrotic cell death. CypD is a component of PTP and a key molecule of cellular necrosis.

5. Apoptosis signal-regulating kinase-1 as a key player in oxidative stress

ASK1, a 160 kDa serine/threonine protein kinase is an ROS-sensitive MAP kinase kinase kinase and activates both p38 and JNK pathways.[42] ASK1 is ubiquitously expressed in most mammalian cells and the kinase activity of ASK1 is activated by many stress signals and proinflammatory cytokines, including H_2O_2, TNF-α, endoplasmic reticulum stress, and serum withdrawal. Thioredoxin 1 binds directly to the N-terminal regulatory domain of ASK1 and inhibits ASK1 activation of this kinase. Upon ROS generation, oxidized thioredoxin 1 is dissociated from ASK1, leading to a robust autophosphorylation of Thr845 in the homo-oligomer.[61] Under modest stressed conditions, activated ASK1 is involved in cardiac hypertrophy, cell protection, and stress responses e.g. cytokine release mediated through the downstream MAP kinase pathways and transcription factors (*Figure 2*).[46,62] We have reported that G-protein-coupled receptor agonists e.g. norepinephrine, angiotensin II, and endothelin rapidly and transiently activate ASK1 via ROS generation and ASK1 is involved in G-protein-coupled receptor agonist-induced NF-κB activation and cardiomyocyte hypertrophy.[43] We have also reported that the ROS–ASK1–JNK pathway plays an important role in apoptosis in the heart under severely stressed conditions.[63] Overexpression of a constitutively active mutant of ASK1 induces apoptosis in isolated rat neonatal cardiomyocytes, whereas neonatal ASK1-deficient cardiomyocytes are resistant to H_2O_2-induced apoptosis. ASK1 is activated in post-infarcted wild-type mouse hearts. Four week after left coronary artery ligation, wild-type hearts had become obviously enlarged compared with ASK1-deficient hearts. The number of apoptotic myocytes after MI is decreased in ASK1-deficient mice.[63] Chronic inhibition of ASK1 activation by transcoronary gene transfer using recombinant adeno-associated virus can attenuate the

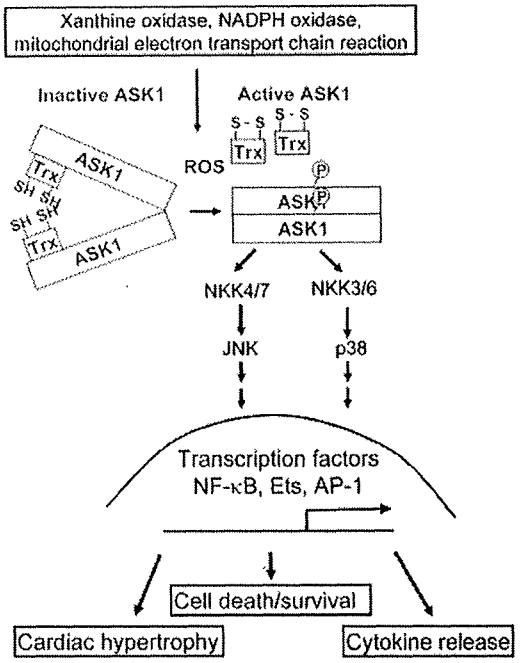

Figure 2 The roles of reactive oxygen species (ROS) and apoptosis signal-regulating kinase-1(ASK1) in oxidative stress. The major sources of ROS in oxidative stress are mitochondria, xanthine oxidase, and NADPH oxidase. The N-terminal regulatory domain of ASK1 interacts with thioredoxin 1 (Trx) in the inactive complex. ROS activate ASK1 mediated by oxidization of Trx and its dissociation from ASK1. Activated ASK1 is involved in cardiac hypertrophy, control of cell fate, and stress responses e.g. cytokine release mediated through the downstream MAP kinase pathways and transcription factors.

progression of cardiac remodelling in TO-2 cardiomyopathic hamsters.[64] In this hamster, inhibition of ASK1 selectively attenuates JNK activation and reduces the number of apoptotic cells. These suggest that the ASK1–JNK pathway may play a pivotal role in regulating LV remodelling by promoting apoptosis.

ASK1–JNK/p38 pathways are also involved in both cell survival and apoptosis. Although the mechanisms have not been clearly understood, the extent and/or duration of activation of JNK/p38 may contribute to determination of cell fate. Sustained activation of JNK/p38 by excessive stimuli may be responsible for apoptosis.[62] In contrast to this hypothesis, we have observed that p38 plays a critical role in the cardiomyocyte survival pathway in cardiac-specific p38α-deficient mice.[65] Although further studies are necessary to clarify the roles of p38 MAP kinase pathways in response to oxidative stresses, it is of interest that the infarct area after ischaemia/reperfusion is dramatically reduced in ASK1-deficient hearts, suggesting that ROS–ASK1 pathway is also involved in necrotic cell death as well as apoptotic cell death.[66] Since ASK1 may be involved in both apoptosis and necrosis, this molecule may be a target of treatment to reduce LV remodelling after MI.

6. Progression of left ventricular remodelling

LV remodelling following MI may promote thinning of the infarcted area and reactive hypertrophic responses of remote myocardium, resulting in progressive enlargement of the LV.[1,67,68] The structure of LV chamber changes from ellipsoidal to spherical shape, i.e. a ratio of long to short axis is decreased. This dilatation is often associated with mitral regurgitation which further deteriorates LV function.[69] Previous studies have also demonstrated that the extent of LV remodelling correlates with prognosis in patients with MI.[3] This is because enlargement of LV chamber is associated with the incidence of cardiac sudden death as well as the chronic HF (CHF).[2]

The thinning of the ventricular wall and chamber dilatation increases the mechanical stress of the ventricular wall and subsequently cause a slippage of the myofibrils. Increased mechanical stress also causes subendocardial ischaemia. Extracellular matrix response to mechanical overload elicits the increase in collagen synthesis which makes the ventricular wall stiffer and thus, increases LV diastolic pressure. There is a large body of clinical evidence that angiotensin-converting enzyme inhibitors, angiotensin receptor antagonists, and β-blockers improve the prognosis of the patients. It should be noted that all these drugs attenuate the progression of LV remodelling and even reverse it.[70–72] Surgical repair of mitral regurgitation could also reverse LV remodelling and improve prognosis.[69,73] Furthermore, surgical volume reduction treatment is performed to improve the symptoms as well as prognosis in CHF.[74,75] Myocardial hibernation or severe myocardial ischaemia by coronary artery narrowings also leads to regional contractile dysfunction, resulting in LV remodelling. This is confirmed by the fact that revascularization to the hibernating or ischaemic myocardium can improve LV function and prevent LV remodelling in patients with post-MI.[76] In contrast to systolic HF, however, diastolic HF is not associated with LV dilatation.[77] In this type of HF, LV wall is often thickened and systolic function is preserved within normal range. This abnormality is frequently observed in elderly people especially associated with hypertension or its history.[78] It is speculated that an increase in myocardial fibrosis and/or myofibrillar stiffening due to myofibrillar hypertrophy may be a major cause of an increase in LV diastolic pressure and thus, pulmonary congestion. There are several reports that oxidative stress is also enhanced in diastolic HF and hypertensive heart disease.[79–81] Thus, oxidative stress may play a pivotal role not only in LV remodelling after MI but also in non-ischaemic LV remodelling due to mechanical overload.

7. Antioxidant and anti-inflammatory therapy for reverse remodelling

Antioxidant and anti-inflammatory treatment may be a promising approach for reverse remodelling. In the transgenic mice of oxidant scavenger SOD, the infarct size following ischaemia/reperfusion is markedly reduced.[15,16] The antioxidant agent, mercaptopropionyl glycine,[82] or edaravone[83] also inhibits cardiac hypertrophy by pressure overload in mice. There has been a plenty of evidence that antioxidant agents attenuate the LV remodelling following MI. Probucol, a potent antioxidant exerts a favourable effect on post-infarction HF in rats,[84,85] adriamycin-induced HF,[86] and tachycardia-induced HF in mongrel dogs.[87] However, not a few experimental studies do not support this hypothesis. Administration of probucol after ligation of coronary artery in rats minimally attenuates interstitial collagen content and does not improve

the prognosis.[88] However, the timing of administration of the antioxidant may be important since another report suggested that the infarct size after ischaemia-reperfusion is significantly influenced by the timing of administration of probucol in Watanabe heritable hyperlipidaemic rabbits.[89]

The dose of the agent may also be critical for antioxidant effect. A small dose of aspirin does not attenuate the inflammatory cytokines. However, a large dose of aspirin exerts an inhibitory effect of inflammatory cytokines although aspirin may not attenuate collagen accumulation and hence, LV remodelling.[90] Collagen synthesis and accumulation may be regulated not only by ROS and inflammatory cytokines but also by other factors, e.g. transforming growth factor-β.[91] Thus, the limited effect of antioxidant may minimally inhibit LV remodelling depending upon the underlying conditions of the heart.

Clinically, vitamin C and E supplementation did not influence cytokine levels, functional indexes, quality of life, or neurohumoral status in patients with advanced CHF.[92–94] HMG-CoA reductase inhibitor, statin, has some pleiotropic effects including antioxidant and anti-inflammatory effects.[95] Although statin can prevent cardiac hypertrophy and apoptotic cell death experimentally, rousvastatin did not improve the prognosis of the patients with CHF in CORONA study[96] and GISSI-HF study.[97] In patients with CHF, plasma levels of inflammatory cytokines are increased.[98] Since the CHF patients with the high levels of cytokines had poor short- and long-term prognosis, anti-TNF therapy using etanercept was evaluated in patients with CHF. However, in RENEWAL study which was combined analysis of medium- and high-dose etanercept vs. placebo, the primary endpoint (death or CHF hospitalization) and the secondary endpoint (death for any cause) were not different between etanercept and placebo.[99] In ATTACH trial, chimeric IgG monoclonal antibody of TNF-α, infliximab did not improve the mortality and morbidity of the patients with CHF. These results suggest that anti-TNF therapy is not effective in treatment of CHF.[100] Etanercept may have an agonistic effect of TNF and infliximab may induce cell lysis by binding of TNF-α–anti TNF-α complex to complements.[101,102] Thus, these anti TNF agents may also have detrimental effects. On the other hand, TNF-α is also an essential molecule for cell survival and thus, it plays a role as a double-edged sword. Anti TNF treatment may be on the critical balance between TNF-α activity and inhibitory potency of anti TNF agents. Dose of drug, timing of administration, and the underlying conditions of the disease may be critically important. Also, underlying conditions of CHF and LV remodelling following MI may not be identical: absence of long-term efficacy of anti-TNF-α treatment may not indicate that anti TNF treatment is ineffective to inhibit LV remodelling after MI. Indeed, etanercept and infliximab are effective in anti-inflammatory action and inhibiting tissue remodelling in rheumatoid arthritis and ankylosing spondylitis.[103–106] To our knowledge, there are no clinical trials of antioxidant drugs combined with anti-cytokine therapy and thus, combined treatment should be tested in future.

The renin–angiotension–aldosterone system (RAAS) has a central role in the pathophysiology of LV remodelling and progression of HF. The pharmacologic inhibition of RAAS attenuates oxidative stress and LV remodelling. Several large trials of angiotensin-converting enzyme inhibitors and angiotensin II type 1 receptor blocker in patients with LV dysfunction or HF after an acute MI were performed and they all demonstrated that the blockade of RAAS reduces the all-cause mortality.[107–110] In these clinical trials, it is also shown that RAAS inhibition attenuates LV remodelling. In animal models with HF, RAAS inhibition demonstrates an attenuation of oxidative stress.[111]

β-blockers can prevent cardiac events and improve the prognosis in patients with acute MI. Carvedilol is a non-selective β-blocker with antioxidant action.[112,113] Administration of carvedilol decreases the oxidative stress level together with improvements of cardiac function in patients with HF.[114] In CAPRICORN study, carvedilol reduced all-cause mortality or non-fatal recurrent MI in patients with LV dysfunction after acute MI.[115] In the echo substudy, carvedilol showed beneficial effects on ventricular remodelling.[116] In the carvedilol or metoprolol European trial (COMET), carvedilol is shown to be superior to metoprolol, suggesting an importance of antioxidant effect.[117] However, the dose and formulation of metoprolol used in this trial has caused a debate, and it has been questioned whether a comparable β1-blockade is obtained in the two intervention groups.[113] Xanthine oxidase is an important source of oxidizing activity molecules and is extensively expressed in patients with HF. Allopurinol effectively counters oxidative stress and attenuates LV remodelling and dysfunction after experimental MI.[118] In clinical setting, allopurinol improves endothelial dysfunction,[119] mortality, and morbidity[120] in patients with CHF. In the OPT-CHF study, a xanthine oxidase inhibitor, oxypurinol, did not exert clinical improvements in unselected patients with moderate-to-severe HF. However, post-hoc analysis suggests that benefits occur in patients with elevated serum uric acid in a manner correlating with the degree of serum uric acid reduction, although prospective clinical studies are necessary.[121]

Thus, several drugs which have beneficial effects on LV remodelling and prognosis in patients with MI and CHF, have some antioxidant effects. However, there is not definitive evidence that antioxidants are effective in reverse remodelling probably because clinically available antioxidant drugs are insufficient in their potency, the dose of the drug is not optimal or the timing of administration is not appropriate in the previous studies. Further studies are needed to clarify the role of oxidative stress in LV remodelling in patients with MI.

8. Conclusion

In acute MI, ROS generated in the ischaemic myocardium directly injure the cell membrane causing cell death. However, ROS also stimulate signal transduction to elaborate inflammatory cytokines which regulate cell survival and cell death in the chain reaction with ROS. In this signal transduction, ASK1, MAP kinase kinase kinase plays a key role in controlling cell fate either in apoptosis or necrosis, and thus, LV remodelling. Chronically, inflammatory cytokines activate MMPs causing a slippage of myofibrils and hence LV dilatation. Since an extent of LV remodelling is a major predictor of prognosis of the patients with MI, therapeutic approach attenuating LV remodelling is critically important. Antioxidant and anti-inflammatory treatments

may be a promising approach though direct positive evidence has not been obtained yet.

Conflict of interest: none declared.

References

1. Pfeffer MA, Braunwald E. Ventricular remodeling after myocardial infarction. Experimental observations and clinical implications. *Circulation* 1990;**81**:1161–1172.
2. White HD, Norris RM, Brown MA, Brandt PW, Whitlock RM, Wild CJ. Left ventricular end-systolic volume as the major determinant of survival after recovery from myocardial infarction. *Circulation* 1987;**76**:44–51.
3. Gaudron P, Eilles C, Kugler I, Ertl G. Progressive left ventricular dysfunction and remodeling after myocardial infarction. Potential mechanisms and early predictors. *Circulation* 1993;**87**:755–763.
4. Frangogiannis NG, Smith CW, Entman ML. The inflammatory response in myocardial infarction. *Cardiovasc Res* 2002;**53**:31–47.
5. Ferdinandy P, Danial H, Ambrus I, Rothery RA, Schulz R. Peroxynitrite is a major contributor to cytokine-induced myocardial contractile failure. *Circ Res* 2000;**87**:241–247.
6. Suematsu N, Tsutsui H, Wen J, Kang D, Ikeuchi M, Ide T *et al.* Oxidative stress mediates tumor necrosis factor-alpha-induced mitochondrial DNA damage and dysfunction in cardiac myocytes. *Circulation* 2003;**107**:1418–1423.
7. Siwik DA, Pagano PJ, Colucci WS. Oxidative stress regulates collagen synthesis and matrix metalloproteinase activity in cardiac fibroblasts. *Am J Physiol Cell Physiol* 2001;**280**:C53–C60.
8. Siwik DA, Colucci WS. Regulation of matrix metalloproteinases by cytokines and reactive oxygen/nitrogen species in the myocardium. *Heart Fail Rev* 2004;**9**:43–51.
9. Peng J, Gurantz D, Tran V, Cowling RT, Greenberg BH. Tumor necrosis factor-alpha-induced AT1 receptor upregulation enhances angiotensin II-mediated cardiac fibroblast responses that favor fibrosis. *Circ Res* 2002;**91**:1119–1126.
10. Kukielka GL, Smith CW, Manning AM, Youker KA, Michael LH, Entman ML. Induction of interleukin-6 synthesis in the myocardium. Potential role in postreperfusion inflammatory injury. *Circulation* 1995;**92**:1866–1875.
11. von Knethen A, Callsen D, Brune B. Superoxide attenuates macrophage apoptosis by NF-kappa B and AP-1 activation that promotes cyclooxygenase-2 expression. *J Immunol* 1999;**163**:2858–2866.
12. Waypa GB, Marks JD, Mack MM, Boriboun C, Mungai PT, Schumacker PT. Mitochondrial reactive oxygen species trigger calcium increases during hypoxia in pulmonary arterial myocytes. *Circ Res* 2002;**91**:719–726.
13. Duilio C, Ambrosio G, Kuppusamy P, DiPaula A, Becker LC, Zweier JL. Neutrophils are primary source of O2 radicals during reperfusion after prolonged myocardial ischemia. *Am J Physiol Heart Circ Physiol* 2001;**280**:H2649–H2657.
14. Scarabelli T, Stephanou A, Rayment N, Pasini E, Comini L, Curello S *et al.* Apoptosis of endothelial cells precedes myocyte cell apoptosis in ischemia/reperfusion injury. *Circulation* 2001;**104**:253–256.
15. Chen Z, Siu B, Ho YS, Vincent R, Chua CC, Hamdy RC *et al.* Overexpression of MnSOD protects against myocardial ischemia/reperfusion injury in transgenic mice. *J Mol Cell Cardiol* 1998;**30**:2281–2289.
16. Wang P, Chen H, Qin H, Sankarapandi S, Becher MW, Wong PC *et al.* Overexpression of human copper, zinc-superoxide dismutase (SOD1) prevents postischemic injury. *Proc Natl Acad Sci USA* 1998;**95**:4556–4560.
17. Irwin MW, Mak S, Mann DL, Qu R, Penninger JM, Yan A *et al.* Tissue expression and immunolocalization of tumor necrosis factor-alpha in postinfarction dysfunctional myocardium. *Circulation* 1999;**99**:1492–1498.
18. Nian M, Lee P, Khaper N, Liu P. Inflammatory cytokines and postmyocardial infarction remodeling. *Circ Res* 2004;**94**:1543–1553.
19. Nakamura K, Fushimi K, Kouchi H, Mihara K, Miyazaki M, Ohe T *et al.* Inhibitory effects of antioxidants on neonatal rat cardiac myocyte hypertrophy induced by tumor necrosis factor-alpha and angiotensin II. *Circulation* 1998;**98**:794–799.
20. Siwik DA, Chang DL, Colucci WS. Interleukin-1beta and tumor necrosis factor-alpha decrease collagen synthesis and increase matrix metalloproteinase activity in cardiac fibroblasts in vitro. *Circ Res* 2000;**86**:1259–1265.
21. Deten A, Holzl A, Leicht M, Barth W, Zimmer HG. Changes in extracellular matrix and in transforming growth factor beta isoforms after coronary artery ligation in rats. *J Mol Cell Cardiol* 2001;**33**:1191–1207.
22. Rohde LE, Ducharme A, Arroyo LH, Aikawa M, Sukhova GH, Lopez-Anaya A *et al.* Matrix metalloproteinase inhibition attenuates early left ventricular enlargement after experimental myocardial infarction in mice. *Circulation* 1999;**99**:3063–3070.
23. Rothstein EC, Byron KL, Reed RE, Fliegel L, Lucchesi PA. H(2)O(2)-induced Ca(2+) overload in NRVM involves ERK1/2 MAP kinases: role for an NHE-1-dependent pathway. *Am J Physiol Heart Circ Physiol* 2002;**283**:H598–H605.
24. Mukherjee SB, Das M, Sudhandiran G, Shaha C. Increase in cytosolic Ca2+ levels through the activation of non-selective cation channels induced by oxidative stress causes mitochondrial depolarization leading to apoptosis-like death in Leishmania donovani promastigotes. *J Biol Chem* 2002;**277**:24717–24727.
25. Oral H, Dorn GW 2nd, Mann DL. Sphingosine mediates the immediate negative inotropic effects of tumor necrosis factor-alpha in the adult mammalian cardiac myocyte. *J Biol Chem* 1997;**272**:4836–4842.
26. Cailleret M, Amadou A, Andrieu-Abadie N, Nawrocki A, Adamy C, Ait-Mamar B *et al.* N-acetylcysteine prevents the deleterious effect of tumor necrosis factor-(alpha) on calcium transients and contraction in adult rat cardiomyocytes. *Circulation* 2004;**109**:406–411.
27. Creemers EE, Cleutjens JP, Smits JF, Daemen MJ. Matrix metalloproteinase inhibition after myocardial infarction: a new approach to prevent heart failure? *Circ Res* 2001;**89**:201–210.
28. Kubota T, McTiernan CF, Frye CS, Slawson SE, Lemster BH, Koretsky AP *et al.* Dilated cardiomyopathy in transgenic mice with cardiac-specific overexpression of tumor necrosis factor-alpha. *Circ Res* 1997;**81**:627–635.
29. Sivasubramanian N, Coker ML, Kurrelmeyer KM, MacLellan WR, DeMayo FJ, Spinale FG *et al.* Left ventricular remodeling in transgenic mice with cardiac restricted overexpression of tumor necrosis factor. *Circulation* 2001;**104**:826–831.
30. Bradham WS, Moe G, Wendt KA, Scott AA, Konig A, Romanova M *et al.* TNF-alpha and myocardial matrix metalloproteinases in heart failure: relationship to LV remodeling. *Am J Physiol Heart Circ Physiol* 2002;**282**:H1288–H1295.
31. Li YY, Feng YQ, Kadokami T, McTiernan CF, Draviam R, Watkins SC *et al.* Myocardial extracellular matrix remodeling in transgenic mice overexpressing tumor necrosis factor alpha can be modulated by anti-tumor necrosis factor alpha therapy. *Proc Natl Acad Sci USA* 2000;**97**:12746–12751.
32. Kinugawa S, Tsutsui H, Hayashidani S, Ide T, Suematsu N, Satoh S *et al.* Treatment with dimethylthiourea prevents left ventricular remodeling and failure after experimental myocardial infarction in mice: role of oxidative stress. *Circ Res* 2000;**87**:392–398.
33. Kameda K, Matsunaga T, Abe N, Hanada H, Ishizaka H, Ono H *et al.* Correlation of oxidative stress with activity of matrix metalloproteinase in patients with coronary artery disease. Possible role for left ventricular remodelling. *Eur Heart J* 2003;**24**:2180–2185.
34. Vanhoutte D, Schellings M, Pinto Y, Heymans S. Relevance of matrix metalloproteinases and their inhibitors after myocardial infarction: a temporal and spatial window. *Cardiovasc Res* 2006;**69**:604–613.
35. Zhao ZQ, Vinten-Johansen J. Myocardial apoptosis and ischemic preconditioning. *Cardiovasc Res* 2002;**55**:438–455.
36. Qin F, Shite J, Liang CS. Antioxidants attenuate myocyte apoptosis and improve cardiac function in CHF: association with changes in MAPK pathways. *Am J Physiol Heart Circ Physiol* 2003;**285**:H822–H832.
37. Suzuki K, Murtuza B, Sammut IA, Latif N, Jayakumar J, Smolenski RT *et al.* Heat shock protein 72 enhances manganese superoxide dismutase activity during myocardial ischemia-reperfusion injury, associated with mitochondrial protection and apoptosis reduction. *Circulation* 2002;**106**:I270–I276.
38. Peng X, Li Y. Induction of cellular glutathione-linked enzymes and catalase by the unique chemoprotective agent, 3H-1,2-dithiole-3-thione in rat cardiomyocytes affords protection against oxidative cell injury. *Pharmacol Res* 2002;**45**:491–497.
39. Cooper D, Stokes KY, Tailor A, Granger DN. Oxidative stress promotes blood cell-endothelial cell interactions in the microcirculation. *Cardiovasc Toxicol* 2002;**2**:165–180.
40. Tritto I, D'Andrea D, Eramo N, Scognamiglio A, De Simone C, Violante A *et al.* Oxygen radicals can induce preconditioning in rabbit hearts. *Circ Res* 1997;**80**:743–748.
41. Hoshida S, Yamashita N, Otsu K, Hori M. The importance of manganese superoxide dismutase in delayed preconditioning: involvement of reactive oxygen species and cytokines. *Cardiovasc Res* 2002;**55**:495–505.

42. Ichijo H, Nishida E, Irie K, ten Dijke P, Saitoh M, Moriguchi T *et al.* Induction of apoptosis by ASK1, a mammalian MAPKKK that activates SAPK/JNK and p38 signaling pathways. *Science* 1997;**275**:90–94.
43. Hirotani S, Otsu K, Nishida K, Higuchi Y, Morita T, Nakayama H *et al.* Involvement of nuclear factor-kappaB and apoptosis signal-regulating kinase 1 in G-protein-coupled receptor agonist-induced cardiomyocyte hypertrophy. *Circulation* 2002;**105**:509–515.
44. Youle RJ, Strasser A. The BCL-2 protein family: opposing activities that mediate cell death. *Nat Rev Mol Cell Biol* 2008;**9**:47–59.
45. Higuchi Y, Otsu K, Nishida K, Hirotani S, Nakayama H, Yamaguchi O *et al.* Involvement of reactive oxygen species-mediated NF-kappa B activation in TNF-alpha-induced cardiomyocyte hypertrophy. *J Mol Cell Cardiol* 2002;**34**:233–240.
46. Takimoto E, Kass DA. Role of oxidative stress in cardiac hypertrophy and remodeling. *Hypertension* 2007;**49**:241–248.
47. Rui T, Kvietys PR. NFkappaB and AP-1 differentially contribute to the induction of Mn-SOD and eNOS during the development of oxidant tolerance. *FASEB J* 2005;**19**:1908–1910.
48. Marsden VS, O'Connor L, O'Reilly LA, Silke J, Metcalf D, Ekert PG *et al.* Apoptosis initiated by Bcl-2-regulated caspase activation independently of the cytochrome c/Apaf-1/caspase-9 apoptosome. *Nature* 2002;**419**:634–637.
49. Ashkenazi A, Dixit VM. Death receptors: signaling and modulation. *Science* 1998;**281**:1305–1308.
50. Chinnaiyan AM, O'Rourke K, Tewari M, Dixit VM. FADD, a novel death domain-containing protein, interacts with the death domain of Fas and initiates apoptosis. *Cell* 1995;**81**:505–512.
51. Hsu H, Xiong J, Goeddel DV. The TNF receptor 1-associated protein TRADD signals cell death and NF-kappa B activation. *Cell* 1995;**81**:495–504.
52. Fiers W, Beyaert R, Declercq W, Vandenabeele P. More than one way to die: apoptosis, necrosis and reactive oxygen damage. *Oncogene* 1999;**18**:7719–7730.
53. Grooten J, Goossens V, Vanhaesebroeck B, Fiers W. Cell membrane permeabilization and cellular collapse, followed by loss of dehydrogenase activity: early events in tumour necrosis factor-induced cytotoxicity. *Cytokine* 1993;**5**:546–555.
54. Festjens N, Vanden Berghe T, Vandenabeele P. Necrosis, a well-orchestrated form of cell demise: signalling cascades, important mediators and concomitant immune response. *Biochim Biophys Acta* 2006;**1757**:1371–1387.
55. Zoratti M, Szabo I. The mitochondrial permeability transition. *Biochim Biophys Acta* 1995;**1241**:139–176.
56. Halestrap AP, McStay GP, Clarke SJ. The permeability transition pore complex: another view. *Biochimie* 2002;**84**:153–166.
57. Crompton M. On the involvement of mitochondrial intermembrane junctional complexes in apoptosis. *Curr Med Chem* 2003;**10**:1473–1484.
58. Tsujimoto Y, Nakagawa T, Shimizu S. Mitochondrial membrane permeability transition and cell death. *Biochim Biophys Acta* 2006;**1757**:1297–1300.
59. Leung AW, Halestrap AP. Recent progress in elucidating the molecular mechanism of the mitochondrial permeability transition pore. *Biochim Biophys Acta* 2008;**1777**:946–952.
60. Nakagawa T, Shimizu S, Watanabe T, Yamaguchi O, Otsu K, Yamagata H *et al.* Cyclophilin D-dependent mitochondrial permeability transition regulates some necrotic but not apoptotic cell death. *Nature* 2005;**434**:652–658.
61. Nishida K, Otsu K. The role of apoptosis signal-regulating kinase 1 in cardiomyocyte apoptosis. *Antioxid Redox Signal* 2006;**8**:1729–1736.
62. Matsuzawa A, Ichijo H. Redox control of cell fate by MAP kinase: physiological roles of ASK1-MAP kinase pathway in stress signaling. *Biochim Biophys Acta* 2008;**1780**:1325–1336.
63. Yamaguchi O, Higuchi Y, Hirotani S, Kashiwase K, Nakayama H, Hikoso S *et al.* Targeted deletion of apoptosis signal-regulating kinase 1 attenuates left ventricular remodeling. *Proc Natl Acad Sci USA* 2003;**100**:15883–15888.
64. Hikoso S, Ikeda Y, Yamaguchi O, Takeda T, Higuchi Y, Hirotani S *et al.* Progression of heart failure was suppressed by inhibition of apoptosis signal-regulating kinase 1 via transcoronary gene transfer. *J Am Coll Cardiol* 2007;**50**:453–462.
65. Nishida K, Yamaguchi O, Hirotani S, Hikoso S, Higuchi Y, Watanabe T *et al.* p38alpha mitogen-activated protein kinase plays a critical role in cardiomyocyte survival but not in cardiac hypertrophic growth in response to pressure overload. *Mol Cell Biol* 2004;**24**:10611–10620.
66. Watanabe T, Otsu K, Takeda T, Yamaguchi O, Hikoso S, Kashiwase K *et al.* Apoptosis signal-regulating kinase 1 is involved not only in apoptosis but also in non-apoptotic cardiomyocyte death. *Biochem Biophys Res Commun* 2005;**333**:562–567.
67. Pfeffer JM, Pfeffer MA, Braunwald E. Influence of chronic captopril therapy on the infarcted left ventricle of the rat. *Circ Res* 1985;**57**:84–95.
68. Opie LH, Commerford PJ, Gersh BJ, Pfeffer MA. Controversies in ventricular remodelling. *Lancet* 2006;**367**:356–367.
69. Otto CM, Clinical practice. Evaluation and management of chronic mitral regurgitation. *N Engl J Med* 2001;**345**:740–746.
70. Abdulla J, Barlera S, Latini R, Kjoller-Hansen L, Sogaard P, Christensen E *et al.* A systematic review: effect of angiotensin converting enzyme inhibition on left ventricular volumes and ejection fraction in patients with a myocardial infarction and in patients with left ventricular dysfunction. *Eur J Heart Fail* 2007;**9**:129–135.
71. Komajda M, Lutiger B, Madeira H, Thygesen K, Bobbio M, Hildebrandt P *et al.* Tolerability of carvedilol and ACE-Inhibition in mild heart failure. Results of CARMEN (Carvedilol ACE-Inhibitor Remodelling Mild CHF EvaluatioN). *Eur J Heart Fail* 2004;**6**:467–475.
72. Lowes BD, Gill EA, Abraham WT, Larrain JR, Robertson AD, Bristow MR *et al.* Effects of carvedilol on left ventricular mass, chamber geometry, and mitral regurgitation in chronic heart failure. *Am J Cardiol* 1999;**83**:1201–1205.
73. Bach DS, Bolling SF. Early improvement in congestive heart failure after correction of secondary mitral regurgitation in end-stage cardiomyopathy. *Am Heart J* 1995;**129**:1165–1170.
74. Franco-Cereceda A, McCarthy PM, Blackstone EH, Hoercher KJ, White JA, Young JB *et al.* Partial left ventriculectomy for dilated cardiomyopathy: is this an alternative to transplantation? *J Thorac Cardiovasc Surg* 2001;**121**:879–893.
75. Athanasuleas CL, Buckberg GD, Stanley AW, Siler W, Dor V, Di Donato M *et al.* Surgical ventricular restoration in the treatment of congestive heart failure due to post-infarction ventricular dilation. *J Am Coll Cardiol* 2004;**44**:1439–1445.
76. Carluccio E, Biagioli P, Alunni G, Murrone A, Giombolini C, Ragni T *et al.* Patients with hibernating myocardium show altered left ventricular volumes and shape, which revert after revascularization: evidence that dyssynergy might directly induce cardiac remodeling. *J Am Coll Cardiol* 2006;**47**:969–977.
77. Zile MR, Baicu CF, Gaasch WH. Diastolic heart failure–abnormalities in active relaxation and passive stiffness of the left ventricle. *N Engl J Med* 2004;**350**:1953–1959.
78. Aurigemma GP, Gaasch WH, Clinical practice. Diastolic heart failure. *N Engl J Med* 2004;**351**:1097–1105.
79. Nishio M, Sakata Y, Mano T, Yoshida J, Ohtani T, Takeda Y *et al.* Therapeutic effects of angiotensin II type 1 receptor blocker at an advanced stage of hypertensive diastolic heart failure. *J Hypertens* 2007;**25**:455–461.
80. Behr TM, Willette RN, Coatney RW, Berova M, Angermann CE, Anderson K *et al.* Eprosartan improves cardiac performance, reduces cardiac hypertrophy and mortality and downregulates myocardial monocyte chemoattractant protein-1 and inflammation in hypertensive heart disease. *J Hypertens* 2004;**22**:583–592.
81. Guo P, Nishiyama A, Rahman M, Nagai Y, Noma T, Namba T *et al.* Contribution of reactive oxygen species to the pathogenesis of left ventricular failure in Dahl salt-sensitive hypertensive rats: effects of angiotensin II blockade. *J Hypertens* 2006;**24**:1097–1104.
82. Date MO, Morita T, Yamashita N, Nishida K, Yamaguchi O, Higuchi Y *et al.* The antioxidant N-2-mercaptopropionyl glycine attenuates left ventricular hypertrophy in in vivo murine pressure-overload model. *J Am Coll Cardiol* 2002;**39**:907–912.
83. Tsujimoto I, Hikoso S, Yamaguchi O, Kashiwase K, Nakai A, Takeda T *et al.* The antioxidant edaravone attenuates pressure overload-induced left ventricular hypertrophy. *Hypertension* 2005;**45**:921–926.
84. Oskarsson HJ, Coppey L, Weiss RM, Li WG. Antioxidants attenuate myocyte apoptosis in the remote non-infarcted myocardium following large myocardial infarction. *Cardiovasc Res* 2000;**45**:679–687.
85. Sia YT, Parker TG, Liu P, Tsoporis JN, Adam A, Rouleau JL. Improved post-myocardial infarction survival with probucol in rats: effects on left ventricular function, morphology, cardiac oxidative stress and cytokine expression. *J Am Coll Cardiol* 2002;**39**:148–156.
86. Siveski-Iliskovic N, Kaul N, Singal PK. Probucol promotes endogenous antioxidants and provides protection against adriamycin-induced cardiomyopathy in rats. *Circulation* 1994;**89**:2829–2835.
87. Nakamura R, Egashira K, Machida Y, Hayashidani S, Takeya M, Utsumi H *et al.* Probucol attenuates left ventricular dysfunction and remodeling

in tachycardia-induced heart failure: roles of oxidative stress and inflammation. *Circulation* 2002;**106**:362–367.
88. Betge S, Lutz K, Roskos M, Figulla HR. Oral treatment with probucol in a pharmacological dose has no beneficial effects on mortality in chronic ischemic heart failure after large myocardial infarction in rats. *Eur J Pharmacol* 2007;**558**:119–127.
89. Hoshida S, Yamashita N, Igarashi J, Aoki K, Kuzuya T, Hori M. Long-term probucol treatment reverses the severity of myocardial injury in watanabe heritable hyperlipidemic rabbits. *Arterioscler Thromb Vasc Biol* 1997;**17**:2801–2807.
90. Adamek A, Hu K, Bayer B, Wagner H, Ertl G, Bauersachs J *et al.* High dose aspirin and left ventricular remodeling after myocardial infarction: aspirin and myocardial infarction. *Basic Res Cardiol* 2007;**102**:334–340.
91. Bujak M, Frangogiannis NG. The role of TGF-beta signaling in myocardial infarction and cardiac remodeling. *Cardiovasc Res* 2007;**74**:184–195.
92. Hennekens CH, Buring JE, Manson JE, Stampfer M, Rosner B, Cook NR *et al.* Lack of effect of long-term supplementation with beta carotene on the incidence of malignant neoplasms and cardiovascular disease. *N Engl J Med* 1996;**334**:1145–1149.
93. Lonn E, Bosch J, Yusuf S, Sheridan P, Pogue J, Arnold JM *et al.* Effects of long-term vitamin E supplementation on cardiovascular events and cancer: a randomized controlled trial. *JAMA* 2005;**293**:1338–1347.
94. Yusuf S, Dagenais G, Pogue J, Bosch J, Sleight P. Vitamin E supplementation and cardiovascular events in high-risk patients. The Heart Outcomes Prevention Evaluation Study Investigators. *N Engl J Med* 2000; **342**:154–160.
95. Takemoto M, Node K, Nakagami H, Liao Y, Grimm M, Takemoto Y *et al.* Statins as antioxidant therapy for preventing cardiac myocyte hypertrophy. *J Clin Invest* 2001;**108**:1429–1437.
96. Kjekshus J, Apetrei E, Barrios V, Bohm M, Cleland JG, Cornel JH *et al.* Rosuvastatin in older patients with systolic heart failure. *N Engl J Med* 2007;**357**:2248–2261.
97. Gissi-Hf I. Effect of rosuvastatin in patients with chronic heart failure (the GISSI-HF trial): a randomised, double-blind, placebo-controlled trial. *Lancet* 2008;**372**:1223–1230.
98. Sharma R, Coats AJ, Anker SD. The role of inflammatory mediators in chronic heart failure: cytokines, nitric oxide, and endothelin-1. *Int J Cardiol* 2000;**72**:175–186.
99. Mann DL, McMurray JJ, Packer M, Swedberg K, Borer JS, Colucci WS *et al.* Targeted anticytokine therapy in patients with chronic heart failure: results of the Randomized Etanercept Worldwide Evaluation (RENEWAL). *Circulation* 2004;**109**:1594–1602.
100. Chung ES, Packer M, Lo KH, Fasanmade AA, Willerson JT. Randomized, double-blind, placebo-controlled, pilot trial of infliximab, a chimeric monoclonal antibody to tumor necrosis factor-alpha, in patients with moderate-to-severe heart failure: results of the anti-TNF Therapy Against Congestive Heart Failure (ATTACH) trial. *Circulation* 2003;**107**: 3133–3140.
101. Evans TJ, Moyes D, Carpenter A, Martin R, Loetscher H, Lesslauer W *et al.* Protective effect of 55- but not 75-kD soluble tumor necrosis factor receptor-immunoglobulin G fusion proteins in an animal model of gram-negative sepsis. *J Exp Med* 1994;**180**:2173–2179.
102. Scallon BJ, Moore MA, Trinh H, Knight DM, Ghrayeb J. Chimeric anti-TNF-alpha monoclonal antibody cA2 binds recombinant transmembrane TNF-alpha and activates immune effector functions. *Cytokine* 1995;**7**:251–259.
103. Weinblatt ME, Kremer JM, Bankhurst AD, Bulpitt KJ, Fleischmann RM, Fox RI *et al.* A trial of etanercept, a recombinant tumor necrosis factor receptor:Fc fusion protein, in patients with rheumatoid arthritis receiving methotrexate. *N Engl J Med* 1999;**340**:253–259.
104. Maini R, St Clair EW, Breedveld F, Furst D, Kalden J, Weisman M *et al.* Infliximab (chimeric anti-tumour necrosis factor alpha monoclonal antibody) versus placebo in rheumatoid arthritis patients receiving concomitant methotrexate: a randomised phase III trial. ATTRACT Study Group. *Lancet* 1999;**354**:1932–1939.
105. Gorman JD, Sack KE, Davis JC Jr. Treatment of ankylosing spondylitis by inhibition of tumor necrosis factor alpha. *N Engl J Med* 2002;**346**: 1349–1356.
106. van der Heijde D, Dijkmans B, Geusens P, Sieper J, DeWoody K, Williamson P *et al.* Efficacy and safety of infliximab in patients with ankylosing spondylitis: results of a randomized, placebo-controlled trial (ASSERT). *Arthritis Rheum* 2005;**52**:582–591.
107. Pfeffer MA, Braunwald E, Moye LA, Basta L, Brown EJ Jr, Cuddy TE *et al.* Effect of captopril on mortality and morbidity in patients with left ventricular dysfunction after myocardial infarction. Results of the survival and ventricular enlargement trial. The SAVE Investigators. *N Engl J Med* 1992;**327**:669–677.
108. The Acute Infarction Ramipril Efficacy (AIRE) Study Investigators. Effect of ramipril on mortality and morbidity of survivors of acute myocardial infarction with clinical evidence of heart failure. *Lancet* 1993;**342**: 821–828.
109. Kober L, Torp-Pedersen C, Carlsen JE, Bagger H, Eliasen P, Lyngborg K *et al.* A clinical trial of the angiotensin-converting-enzyme inhibitor trandolapril in patients with left ventricular dysfunction after myocardial infarction. Trandolapril Cardiac Evaluation (TRACE) Study Group. *N Engl J Med* 1995;**333**:1670–1676.
110. Pfeffer MA, McMurray JJ, Velazquez EJ, Rouleau JL, Kober L, Maggioni AP *et al.* Valsartan, captopril, or both in myocardial infarction complicated by heart failure, left ventricular dysfunction, or both. *N Engl J Med* 2003;**349**:1893–1906.
111. Khaper N, Singal PK. Modulation of oxidative stress by a selective inhibition of angiotensin II type 1 receptors in MI rats. *J Am Coll Cardiol* 2001;**37**:1461–1466.
112. Arumanayagam M, Chan S, Tong S, Sanderson JE. Antioxidant properties of carvedilol and metoprolol in heart failure: a double-blind randomized controlled trial. *J Cardiovasc Pharmacol* 2001;**37**:48–54.
113. Kveiborg B, Major-Petersen A, Christiansen B, Torp-Pedersen C. Carvedilol in the treatment of chronic heart failure: lessons from the Carvedilol Or Metoprolol European Trial. *Vasc Health Risk Manag* 2007;**3**:31–37.
114. Nakamura K, Kusano K, Nakamura Y, Kakishita M, Ohta K, Nagase S *et al.* Carvedilol decreases elevated oxidative stress in human failing myocardium. *Circulation* 2002;**105**:2867–2871.
115. Dargie HJ. Effect of carvedilol on outcome after myocardial infarction in patients with left-ventricular dysfunction: the CAPRICORN randomised trial. *Lancet* 2001;**357**:1385–1390.
116. Doughty RN, Whalley GA, Walsh HA, Gamble GD, Lopez-Sendon J, Sharpe N. Effects of carvedilol on left ventricular remodeling after acute myocardial infarction: the CAPRICORN Echo Substudy. *Circulation* 2004;**109**:201–206.
117. Poole-Wilson PA, Swedberg K, Cleland JG, Di Lenarda A, Hanrath P, Komajda M *et al.* Comparison of carvedilol and metoprolol on clinical outcomes in patients with chronic heart failure in the Carvedilol Or Metoprolol European Trial (COMET): randomised controlled trial. *Lancet* 2003;**362**:7–13.
118. Engberding N, Spiekermann S, Schaefer A, Heineke A, Wiencke A, Muller M *et al.* Allopurinol attenuates left ventricular remodeling and dysfunction after experimental myocardial infarction: a new action for an old drug? *Circulation* 2004;**110**:2175–2179.
119. Farquharson CA, Butler R, Hill A, Belch JJ, Struthers AD. Allopurinol improves endothelial dysfunction in chronic heart failure. *Circulation* 2002;**106**:221–226.
120. Struthers AD, Donnan PT, Lindsay P, McNaughton D, Broomhall J, MacDonald TM. Effect of allopurinol on mortality and hospitalisations in chronic heart failure: a retrospective cohort study. *Heart* 2002;**87**: 229–234.
121. Hare JM, Mangal B, Brown J, Fisher C Jr, Freudenberger R, Colucci WS *et al.* Impact of oxypurinol in patients with symptomatic heart failure. Results of the OPT-CHF study. *J Am Coll Cardiol* 2008;**51**: 2301–2309.

平成21年1月23日発行（年6回／1,3,5,7,9,11,隔月発行）第24巻1号（通巻第123号）　ISSN 0913-5006 CODEN:DDSYEI

Drug Delivery System

Official Journal of the Japan Society of Drug Delivery System

PUBLISHED BIMONTHLY

2009 VOL.24 JAN. NO. 1